Characteristics of Hawaiian Volcanoes
Editors: Michael P. Poland, Taeko Jane Takahashi, and Claire M. Landowski
U.S. Geological Survey Professional Paper 1801, 2014

Chapter 8

The Dynamics of Hawaiian-Style Eruptions: A Century of Study

By Margaret T. Mangan[1], Katharine V. Cashman[2], and Donald A. Swanson[1]

Abstract

This chapter, prepared in celebration of the Hawaiian Volcano Observatory's centennial, provides a historical lens through which to view modern paradigms of Hawaiian-style eruption dynamics. The models presented here draw heavily from observations, monitoring, and experiments conducted on Kīlauea Volcano, which, as the site of frequent and accessible eruptions, has attracted scientists from around the globe. Long-lived eruptions in particular—Halemaʻumaʻu 1907–24, Kīlauea Iki 1959, Mauna Ulu 1969–74, Puʻu ʻŌʻō-Kupaianaha 1983–present, and Halemaʻumaʻu 2008–present—have offered incomparable opportunities to conceptualize and constrain theoretical models with multidisciplinary data and to field-test model results. The central theme in our retrospective is the interplay of magmatic gas and near-liquidus basaltic melt. A century of study has shown that gas exsolution facilitates basaltic dike propagation; volatile solubility and vesiculation kinetics influence magma-rise rates and fragmentation depths; bubble interactions and gas-melt decoupling modulate magma rheology, eruption intensity, and plume dynamics; and pyroclast outgassing controls characteristics of eruption deposits. Looking to the future, we anticipate research leading to a better understanding of how eruptive activity is influenced by volatiles, including the physics of mixed CO_2-H_2O degassing, gas segregation in nonuniform conduits, and vaporization of external H_2O during magma ascent.

Introduction

> Tonight in presence of the firepit, with the glowing lava again gushing and pounding and shaking the seismographs, I am asked to tell you something of the scientific meaning of it.
>
> —*Thomas A. Jaggar, Jr.* (1945)

Of endless fascination to the observers of Hawaiian eruptions is the "marvelous. . . superlative mobility" of molten lava (Perret, 1913a). This observation is fundamental, for ultimately the fluidity of basaltic magma is what distinguishes the classic Hawaiian-style eruption from other forms of volcanism. Eruption of free-flowing tholeiitic basalt feeds the iconic images of Hawaiian curtains of fire, lava fountains, lava lakes, Pele's hair, and thread-lace scoria (fig. 1). Moreover, thin flows of fluid basalt are central to Hawaiian shield building, requiring quasi-steady-state magma supply and throughput for hundreds of thousands of years.

Early observations of the eruptive activity at Kīlauea and Mauna Loa volcanoes demonstrated that their broad, shield-like shape results chiefly from rift-zone eruptions fed from a summit magma reservoir and that the summit reservoir itself comprises interconnected storage regions that fill and drain repeatedly (for example, Eaton and Murata, 1960; Eaton, 1962; Fiske and Kinoshita, 1969; Wright and Fiske, 1971).

The classic Hawaiian-style eruption typically initiates with a fissure emanating from en echelon fractures formed as a dike propagates across the caldera floor or down the rift zone from the main magma-storage region. Within hours to days, parts of the fissure seal off and focus the eruption into a solitary lava fountain towering tens to hundreds of meters above a central vent. A rain of molten pyroclasts splashes down around the vent, feeding rootless lava flows that spread across the landscape. The incandescence of liquid rock is what draws the eye of the observer, but it is actually a subordinate player, with the volume of magmatic gas erupted exceeding the volume of lava by as much as 70 to 1 (Greenland and others, 1988).

Once established, a central vent may host many fountaining episodes. New episodes start with a column of lava quietly rising in the conduit. Its upward progression is punctuated by rhythmic rise and fall as trapped gas is released. Low dome fountains appear, building to a steady, high fountain over minutes to hours. Fountaining episodes may persist for hours to days, discharging lava at rates of a few hundred cubic meters per second. In contrast to their slow buildup, fountain episodes quit abruptly, ending in chaotic bursts of gas and dense spatter as lava ponded around the vent is swallowed back down into the conduit.

[1]U.S. Geological Survey.
[2]University of Bristol, U.K.

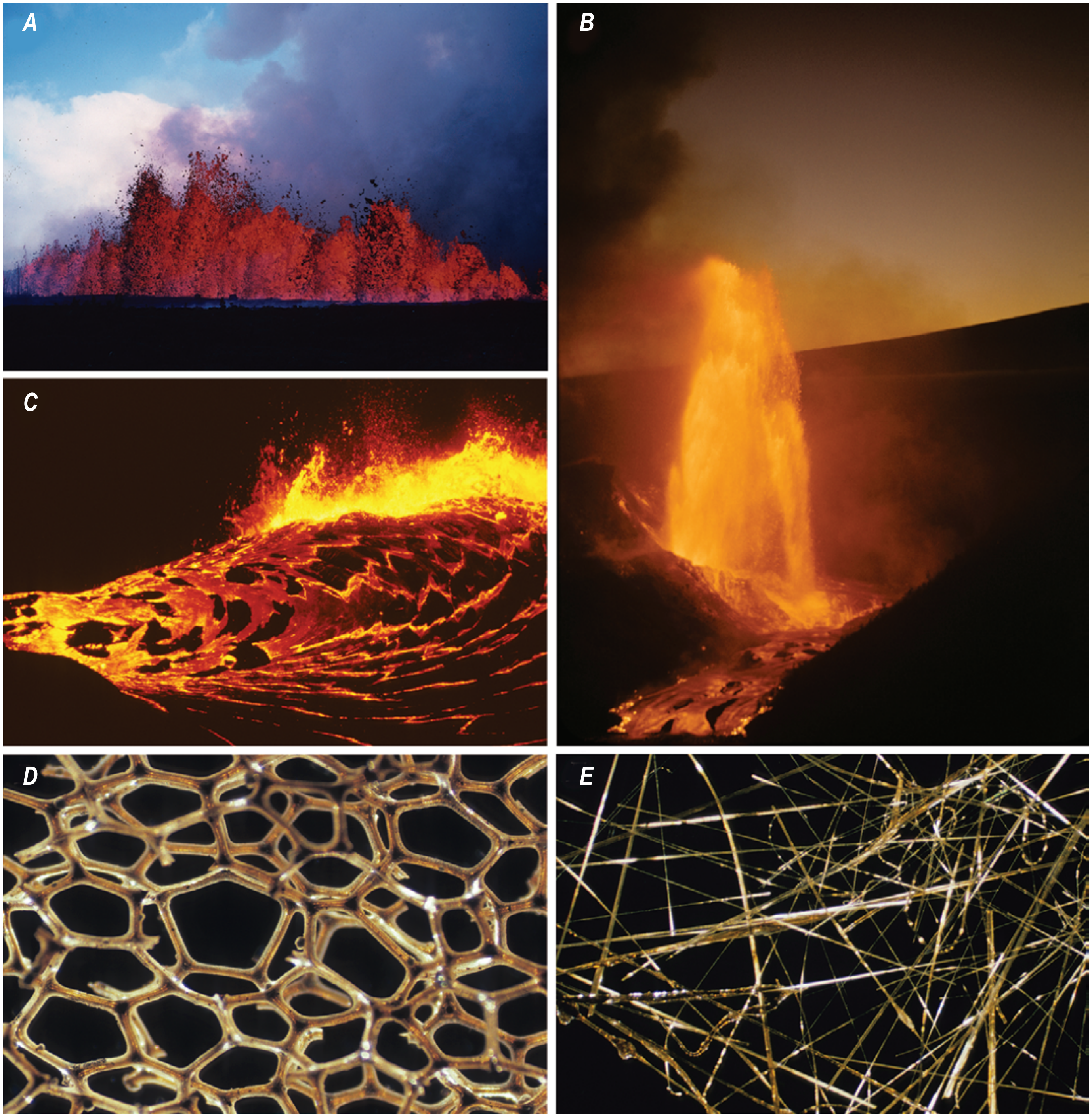

Figure 1. Fluidity of basalt at near-liquidus temperatures is revealed in fountains of molten rock, spattering lava lakes, delicate magmatic foams, and spun glass filaments of classic Hawaiian-style eruptions. *A*, 60- to 100-m-high fountains from a fissure eruption in 1983, showing a 500-m-long segment of an eruptive fissure that extended 1 km along the East Rift Zone. Photograph by J.D. Griggs. *B*, 320-m-high lava fountain from first phase of the 1959 Kīlauea Iki eruption at Kīlauea's summit. Molten fallback from fountain feeds a river of lava 90 m wide. Photograph by J.P. Eaton. *C*, Mauna Ulu lava lake in September 1972. Lake circulation is from left to right, with 5- to 10-m-high spattering occurring at lake margin, where pliable lava crust circulates downward. Lava-lake circulation patterns were vividly described by Jaggar (1917): ". . . crusts form, thicken and stream across the lava lake to founder with sudden tearing, downsucking, flaming and violent effervescence. . . ." Photograph by R.I. Tilling. *D*, Delicate structure of thread-lace scoria (reticulite), a term coined by J.D. Dana after visiting Kīlauea in 1887 (Dana, 1890). View through a 5X binocular microscope reveals an open honeycomb of polygonal cells. Bubble walls (films) thin to the point of rupture as gas expands, leaving a rapidly quenched skeleton of glass struts, trigonal in cross section (plateau borders) and ~0.05 mm thick, that meet to mark original foam structure created during high lava fountaining. Photograph by M.T. Mangan. *E*, Pele's hair (spun volcanic glass) as viewed through a 5X binocular microscope. Molten drops of basaltic lava are stretched into long glass filaments, <0.5 mm in diameter and as much as 0.5 m long, in turbulent updrafts surging above active vents and skylights in lava tubes. Photograph by M.T. Mangan.

An epoch of episodically occurring lava fountains eventually closes with diminished fountain heights and declining discharge rates. The end of fountain activity may signal the end of an eruption or, alternatively, the beginning of steady, effusive activity from an open vent or lava lake. Early accounts of lava-lake dynamics used vivid language, describing “terrific ebullitions,” “splashing sinkholes,” “floating islands,” “thin skins,” and “plastic crusts” as the stuff of Halemaʻumaʻu lava lake. In today’s vernacular, the salient features include a lake-bottom feeder conduit driving sporadic surface spattering and (or) low fountains at the surface; complex, lake-wide circulation patterns; and rhythmic rise-fall cycles associated with accumulation of gas bubbles.

In this chapter, we provide the reader with a historical perspective on how we came to know what we know of the dynamics of Hawaiian-style eruptions, ending with an eye toward what is yet to be learned. As the site of the Hawaiian Volcano Observatory (HVO) and home to frequent, accessible eruptions, Kīlauea Volcano (fig. 2) has played a pivotal role in shaping research and technological innovation. It is thus fitting that we start with an overview of milestone Kīlauea eruptions that have fed our evolving understanding of how volcanoes work.

Halemaʻumaʻu 1907–24

From 1907 until 1924, scientific research at Kīlauea Volcano centered on the persistent lava lake within Halemaʻumaʻu, laying the groundwork for the first models of magmatic convection and open-system degassing. Daly (1911) and Perret (1913b) envisioned cellular convection in the lake, with buoyant upwelling of bubble-rich magma and dense, degassed lava sinking with much spattering and sloshing at the opposite end. These early workers realized that exchange flow was required to supply the heat necessary for persistent activity, but they differed in their views of the geometry and composition of exchange flow—whether gas-charged magma or gas alone was exchanged, and whether convection cells were confined to the lake or penetrated deeper into the conduit. Perret (1913b), in particular, emphasized open-system degassing as critical to lake circulation, arguing that downwelling of degassed lava creates a “powerful siphon effect that is the mainspring of the circulatory system” and suggesting that descending lava is “re-heated and re-vivified” by infusion of minute gas bubbles rising from the depths of the conduit. Geophysical and geochemical investigations of recent lava lakes (Swanson and others, 1979; Tilling and others, 1987;

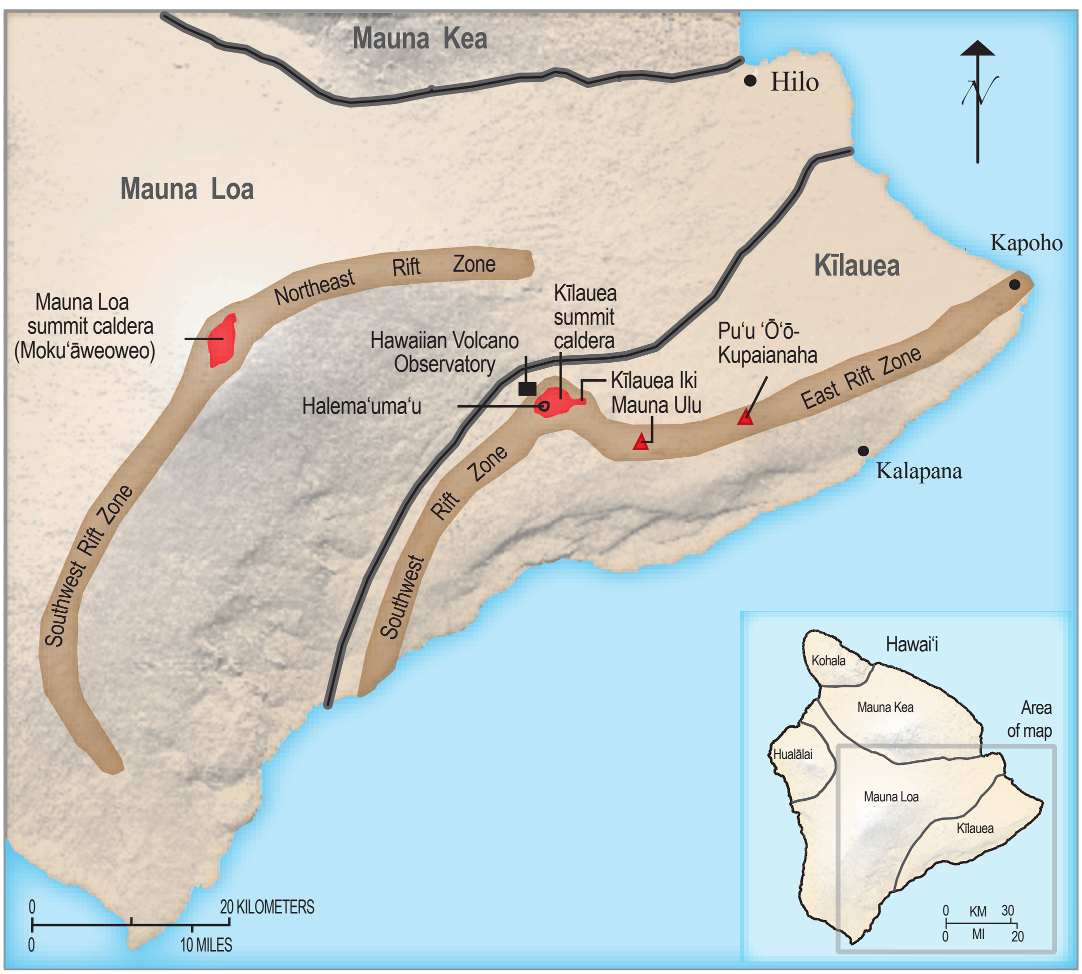

Figure 2. Sketch map of southeastern Hawaiʻi, showing summit calderas and rift zones of Mauna Loa and Kīlauea volcanoes and locations of the Hawaiian Volcano Observatory (HVO) and Kīlauea’s Halemaʻumaʻu, Kīlauea Iki, Mauna Ulu, and Puʻu ʻŌʻō-Kupaianaha eruptive vents. Modified from Babb and others (2011).

Johnson and others, 2005; Patrick and others, 2011a; Orr and Rea, 2012) have pursued the role of open-system degassing in controlling lake activity and longevity and have opened the door to new questions on how and where gas accumulates in shallow plumbing systems and on the mode of gas release.

Kīlauea Iki 1959

The Kīlauea Iki summit eruption marked a major milestone in HVO's history (Eaton and Murata, 1960; Murata, 1966; Murata and Richter, 1966; Richter and Moore, 1966; Richter and Murata, 1966; Richter and others, 1970; see Helz and others, this volume, chap. 6). This spectacular eruption was preceded by an intense swarm of deep (45–60 km) earthquakes and followed by weak tremor in the middle crust and then inflation at the summit. Within 3 months of the onset of deep seismicity, a fissure erupted high on the wall of Kīlauea Iki pit crater. Over 36 days, 17 unusually high and hot fountaining episodes filled the pit crater below with 37 million m^3 of picritic basalt. Fountaining episodes terminated abruptly when the level of the lava lake reached, then flooded, the vent.

The arrival of new staff and modernization of the monitoring network just before the Kīlauea Iki eruption gave HVO an unprecedented opportunity for comprehensive monitoring of the eruption. For the first time, the course of magma—from mantle source to surface vent—could be quantitatively charted by migrating earthquakes, ground deformation, and lava extrusion. A systematic program of lava sampling and measurements of fountain height, discharge rate, and lava temperature provided data critical to constraining later eruption dynamics models.

Mauna Ulu 1969–74

The nearly 5-year-long Mauna Ulu eruption gave HVO staff their first opportunity to study long-lived rift-zone volcanism (Peterson and others, 1976; Swanson and others, 1979; Tilling and others, 1987). Mauna Ulu's repertoire was diverse, including 12 episodic lava-fountain events, near-continuous lava-lake activity, shield building, lava tube formation, and littoral lava-seawater interactions along Hawai‘i's south coastline. The final 2 years of the eruption were punctuated by brief outbursts from fissures opening uprift of the Mauna Ulu vent, including a 3-day eruption at the summit.

Throughout the eruption, seismicity and deformation at Kīlauea's summit correlated with events at the Mauna Ulu vent, providing new insight into how summit-reservoir overpressure is balanced by waxing and waning eruptive output. The term "gas pistoning" was coined during the Mauna Ulu eruption to describe cyclic degassing bursts that produced slow rise and rapid fall of the lava column (Swanson and others, 1979; Tilling and others, 1987). Rise-fall cycles typically occurred over tens of minutes to a few hours. The surface of the lava lake is relatively calm during the rise in a cycle but erupts into vigorous bubbling and spattering as gas escapes and the lava level drops. These observations, which have fueled numerous laboratory experiments and numerical models for two-phase flow, provide a conceptual link between the dynamics of Hawaiian and Strombolian eruption styles.

Pu‘u ‘Ō‘ō-Kupaianaha and Halema‘uma‘u 1983–Present

The present Pu‘u ‘Ō‘ō-Kupaianaha eruption marks the most voluminous outpouring of lava on Kīlauea's East Rift Zone since the 15th century and is the longest East Rift Zone eruption ever recorded (see descriptions by Wolfe and others, 1987, 1988; Heliker and Wright, 1991; Heliker and Mattox, 2003; Poland and others, 2008). Five main epochs capture the diverse and sometimes destructive characteristics of this extraordinary eruption. The first epoch began in January 1983 with 24 hours of migrating earthquakes and ground deformation as a dike from Kīlauea's summit propagated down the East Rift Zone. The dike, traveling 550 m/h laterally and 70 m/h vertically, breached the surface in a linear series of fissures 8 km long (Wolfe and others, 1987). Within 5 months, the fissure eruption had localized to a single vent, Pu‘u ‘Ō‘ō, that hosted more than 3 years of remarkably regular episodic lava fountains.

In July 1986, after 44 episodes of high fountaining, the conduit beneath Pu‘u ‘Ō‘ō ruptured. Thus began a second epoch characterized by quasi-steady effusion from Kupaianaha vent, 3 km downrift of Pu‘u ‘Ō‘ō. The next 5½ years saw construction of a broad shield with a summit lava lake and a well-developed lava tube system that efficiently delivered flows from Kupaianaha to the coastline, igniting dramatic littoral activity and overrunning much of the community of Kalapana. Starting in mid-1990, Kupaianaha entered a protracted stage of diminishing output and frequent pauses (Kauahikaua and others, 1996). Kupaianaha's slow decline revitalized Pu‘u ‘Ō‘ō. By February 1992, Kupaianaha's activity had ceased, and the eruption was back at Pu‘u ‘Ō‘ō, starting the third epoch.

Over the next 15 years, effusion of lava from Pu‘u ‘Ō‘ō was nearly continuous, interrupted only temporarily by nearby fissure eruptions and East Rift Zone intrusions (particularly in 1997, 1999, and 2007). In July 2007, the eruption moved down the rift zone again to a site between Pu‘u ‘Ō‘ō and Kupaianaha, starting the fourth epoch. Effusion from this vent lasted until March 2011 and again sent lava into Kalapana, causing additional destruction. Like Kupaianaha, effusion from that vent eventually waned, ending in March 2011, when another brief East Rift Zone fissure eruption occurred. The fifth, currently ongoing (as of September 2014) epoch has been marked by a return to effusion from Pu‘u ‘Ō‘ō after that fissure eruption.

In March 2008, an eruptive vent also opened at Kīlauea's summit (Houghton and others, 2011; Swanson and others, 2011). Pu‘u ‘Ō‘ō still pumps out lava on the rift zone, but in addition, a lava lake circulates within the recesses of a crater on the east margin of Halema‘uma‘u Crater within Kīlauea Caldera (Patrick and others, 2011a, 2013). First appearing as a fuming, incandescent crack, the new vent evolved by way of a series of magmatic gas blasts during 2008 and 2011 into an active lava lake more than 100 m in diameter. As of this writing (September 2014), neither vent shows any sign of shutting down.

The East Rift Zone eruption, which celebrated its 31st year in January 2014, has seen the introduction of new, sophisticated technology and a steady influx of scientists from diverse disciplines. Major efforts have gone into interpreting integrated datasets from state-of-the-art geophysical and geochemical sensors. Perhaps most significant in this period of rapidly evolving capabilities, at least from the perspective of eruption dynamics, is the initiation of systematic gas monitoring just before the start of the Puʻu ʻŌʻō eruption. Valuable volcanic gas samples were collected during the 1912–24 Halemaʻumaʻu activity (Jaggar, 1940; reanalyzed by Gerlach, 1980), but thereafter, only a few sporadic samples were obtained. Not until the installation of HVO's gas-analysis laboratory in 1980 did monitoring of volcanic gases take a prominent role, alongside monitoring of ground deformation and earthquakes, in building the conceptual framework upon which models of magma transport and eruption are built (see sections below entitled "Geochemistry of Degassing" and "Overview of Existing Eruption Models," as well as Sutton and Elias, this volume, chap. 7).

Magma Transport

> The continuance of eruption at any point depends on victory in the *struggle with cold*.
>
> —*Reginald A. Daly* (1911)

Early 20th century volcanologists recognized that magma came to the surface through dike propagation. Observing relict gas cavities in the tops of exhumed laccoliths exposed in the western United States, Daly (1911) postulated a "blowpipe" mechanism for dike propagation in which hot, caustic gases digested rock strata in advance of rising magma. Perret (1913c) similarly proposed gas-driven "trepanning" and "stoping" of a "vertical tunnel" in overlying strata through which buoyant magma could pass (figs. 3*A*,*B*).

Later field observations in Hawaiʻi, particularly on the Island of Oʻahu, supplied data on the size, shape, and orientation of dikes, providing the first quantitative framework for modeling the delivery of basaltic magma to the surface (Stearns and Vaksvik, 1935; Stearns, 1939; Wentworth and Jones, 1940; Wentworth and Macdonald, 1953). Blade-shaped dikes a few meters thick emerged as "typical" of Hawaiian volcanic systems. Stearns and Vaksvik (1935), working in the eroded Koʻolau shield on Oʻahu, may have been the first to use the term "dike complex" in Hawaiʻi to describe the recurrence of near-vertical preferred pathways, citing traverses with as many as 100 dikes in 1 mile.

At mid-century, a dynamic picture of magma transport emerged from seismic and deformation networks installed just before the 1959 Kīlauea Iki eruption. The results were described by J.P. Eaton, twice director of HVO, who used patterns of earthquake and ground deformation to construct a working model of Kīlauea that charted the "course of magma as it accumulates in a shallow reservoir within the volcano and as it migrates from this reservoir into the rift zones" (Eaton, 1962). Eaton's conceptualization provided the framework needed to apply theoretical fracture mechanics, fluid dynamics, and thermodynamics to the problem of magma transport in Hawaiʻi.

Mechanics of Dike Propagation

Time scales of shallow dike injections are sufficiently short to be observed directly (hours to days), so that as HVO's monitoring networks became more robust, geophysical data fostered many studies of dike propagation. Studies coupling classical fracture mechanics with the physics of fluid flow were conducted, integrating the driving forces of magma pressure and buoyancy with the resisting force of rock tensile strength.

Hydraulic fracturing of rock during shallow dike propagation at Kīlauea requires magma pressures of 2 to 10 MPa (Aki and others, 1977; Rubin and Pollard, 1987). Stress concentration at the dike tip is the leading wedge for crack initiation (fig. 3*C*). Studies by Rubin and Pollard (1987), Lister and Kerr (1991), and Rubin (1993) suggested that a vanguard of gas is as important as magma pressure in dike propagation, but not as the blowpipe that Daly and his contemporaries postulated at the beginning of the century. Instead, microfractures in the damage zone at the dike tip are infiltrated by low-viscosity aqueous fluid (either exsolved magmatic volatiles or external pore fluids). Pressurized microcracks lower the effective tensile strength of the rock and coalesce, creating larger cracks into which the more viscous fluid (magma) can penetrate to extend and widen the dike. Ryan (1988) used a finite-element model to show that a tensile stress regime exists at the dike tip and a compressive stress regime at the margins where the dike is widening. Seismicity associated with dike propagation was attributed to stress release in zones of compression (Aki and others, 1977; Klein and others, 1987). As the surface is approached, overburden pressure decreases, causing torsion of the local principal stresses and segmentation of the dike tip (Pollard, 1973; Hill, 1977; Delaney and Pollard, 1981; Pollard and others, 1982; Rubin and Pollard 1987; Ryan, 1988) and resulting in an en echelon set of eruptive fissures—the signature opening stage of Hawaiian-style eruptions (fig. 3*D*).

Thermodynamics of Magma Flow in Dikes and Fissures

Ryan (1988) described the thermodynamics of dike propagation at Kīlauea as a process of natural selection by which only the "fortunate dikes" traversing the hot, central core of the magma complex make it to the surface before freezing. His assertion is supported by the dikes exposed in the Koʻolau complex, which generally intrude along the margins, or median axis, of earlier, but still hot, dikes (fig. 4).

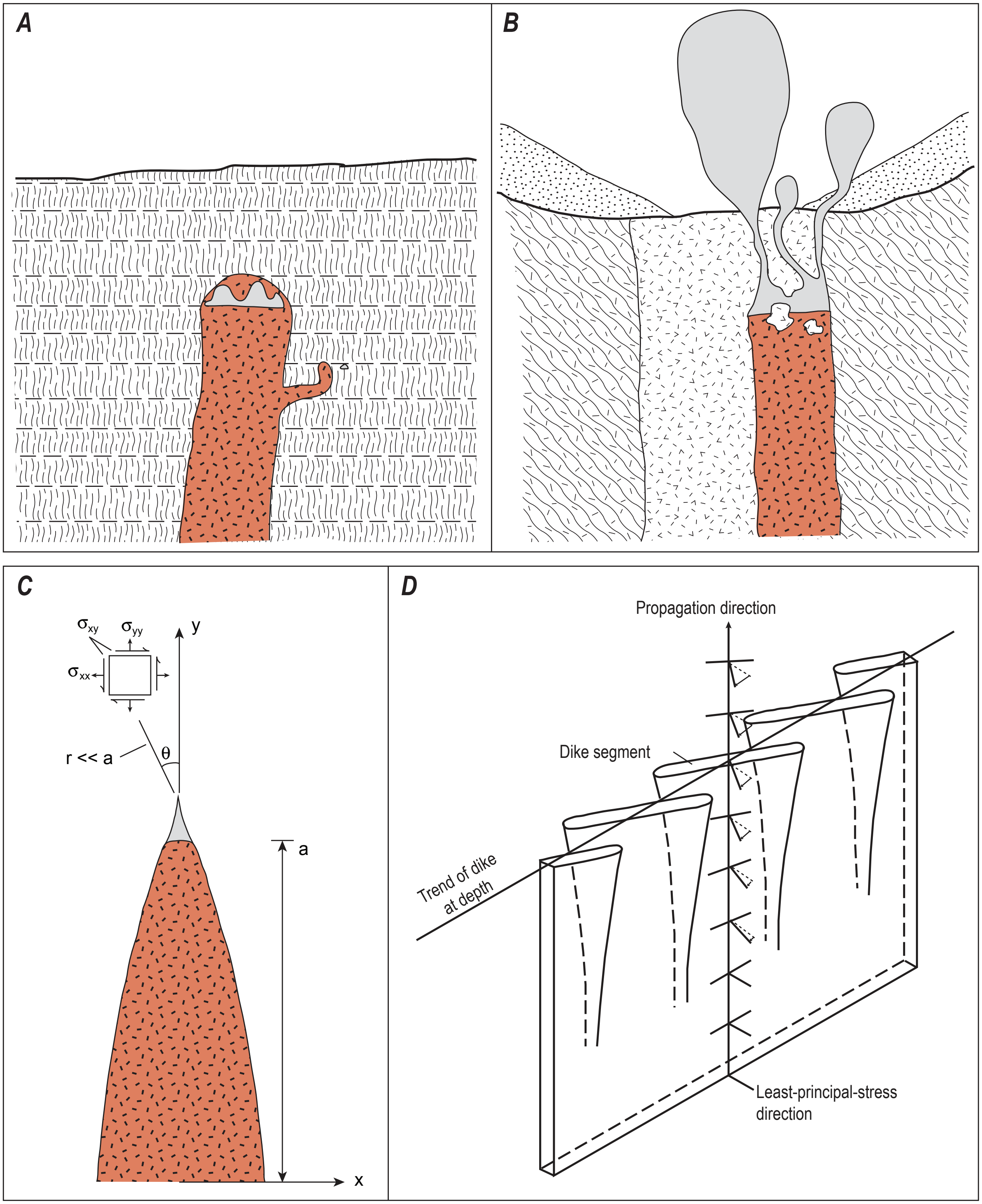

Figure 3. Past (*A,B*) versus present (*C,D*) conceptualizations of basaltic dike propagation. Past conceptualizations (modified from Perret, 1913c, and Daly, 1911), show lava columns capped with hot, compressed gas (gray shading) fluxing (*A*) and stoping (*B*) paths to surface. Present conceptualizations *C* and *D* (modified from Rubin and Pollard, 1987, and Delaney and Pollard, 1981, respectively) illustrate application of modern fracture mechanics. In figure 3*C*, σ is the orthogonal (xx,yy) and oblique (xy) stress component at dike tip along ray path, *r*, at an angle θ from vertical dike axis for *r*<<*a*, where *a* is dike half-length. Gray shading represents a vanguard of low-viscosity fluid (volatiles). Part *D* illustrates near-surface, en echelon segmentation of a rising tabular dike due to rotation in a plane perpendicular to propagation direction (least-principal-stress direction).

Likewise, dike intensity (percentage of host rock occupied by dikes) drops precipitously outside the thermal core of the dike complex—in the Koʻolau complex it decreases from 50–70 to <5 percent over a few hundred meters (Walker, 1987). Helz and others (in press and this volume, chap. 6) used olivine-glass geothermometry of rapidly quenched pyroclasts to infer ambient temperatures of 1,145–1,235 °C within the active dike-and-sill complex at Kīlauea's summit.

The first thermodynamic models avoided the complexities of multiple dike injection and treated the problem of a single dike invading cold country rock under conditions of steady magma supply (Delaney and Pollard, 1982; Hardee, 1987; Bruce and Huppert, 1989, 1990). The initial heat exchange creates a layer of congealed magma along the walls of the dike, confining flow to its central region. The growth of the congealed zone and eventual freezing of the magma hinges on the balance between heat conducted out of the walls of the dike and advected in the direction of flow. Using typical values for dike thickness, magma pressure, magma temperature, viscosity, and magma-flow rates, models for Kīlauea predict that magma flowing a few kilometers from its source should freeze within hours of emplacement, assuming a normal geothermal gradient. Successful propagation of a dike to the surface therefore requires that it follow a thermal "hot zone" built from decades, if not centuries, of intrusive activity. Thermodynamic models of Kīlauea's upper East Rift Zone (Hardee, 1987) suggest that an intrusive flux of ~10^{-3} km^3/y over a span of 2–3 decades is required to form hot pathways for aseismic magma transport without brittle fracture.

The dikes that do breach the surface to feed fissure eruptions face additional heat loss through radiation, which increases as the fourth power of absolute temperature. Initial fissure sections shut down within hours to a few days of opening as the pressure driving magma flow diminishes, or because the magma-transport pathways focus at one or a few central vents. Numerical models (Delaney and Pollard, 1982; Bruce and Huppert, 1989, 1990; Wylie and others, 1999) indicate that focusing the flow of magma from an initial linear

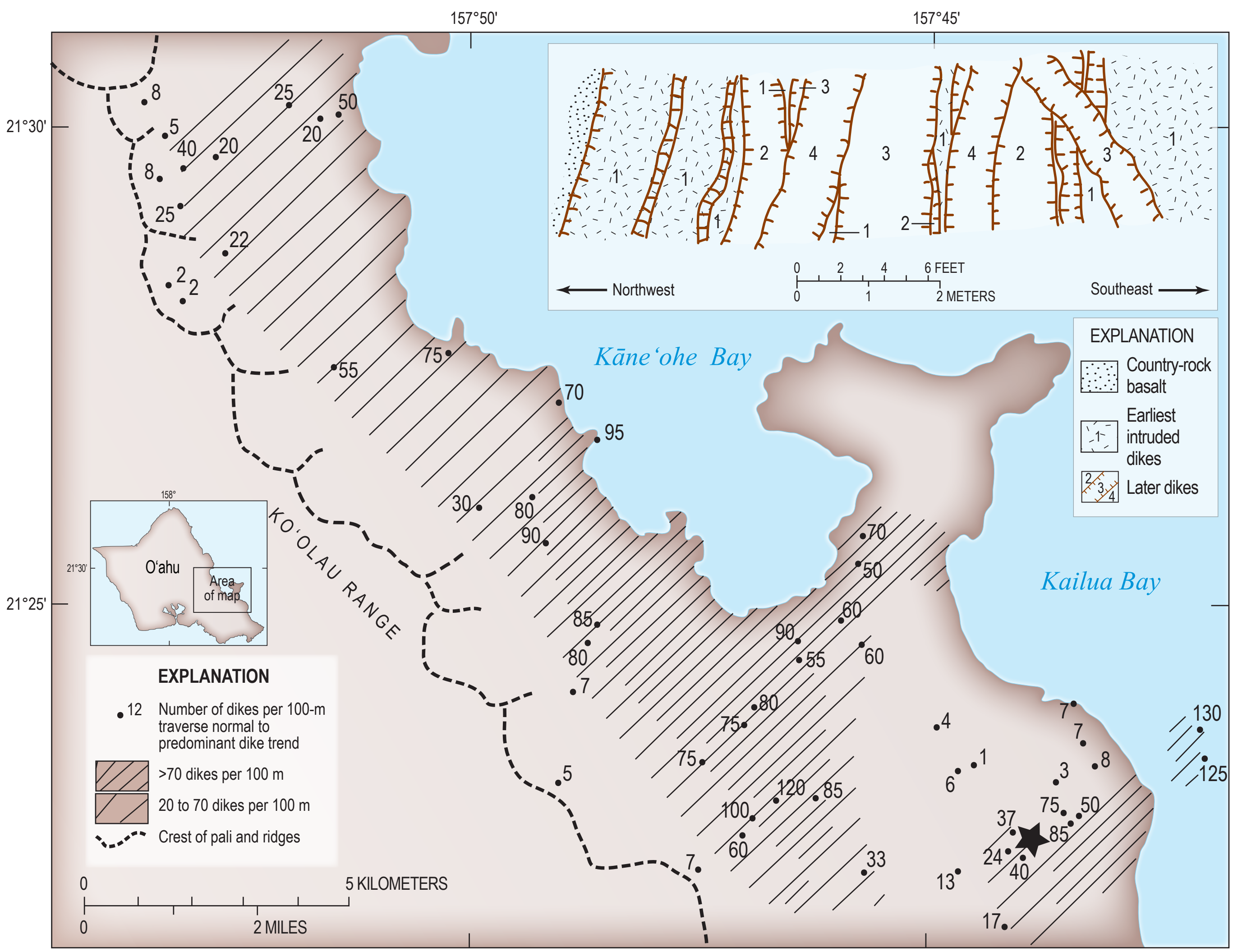

Figure 4. Sketch map showing high concentration of basaltic dikes composing the "paleo hot zone" in eroded core of Koʻolau volcano in eastern Oʻahu. G.P.L. Walker mapped 7,400 subparallel dikes totaling 3 to 5 km in thickness in widest part of complex. Inset (area denoted by star) shows part of a succession of 14 intrusions across an outcrop 13.6 m wide. Modified from Walker (1987).

geometry to one or a few central vents strongly depends on fissure geometry. When the fissure varies in width, advective heat is reduced within narrow sections, owing to lower flow rates. Reduced heat advection promotes solidification, which contributes to further narrowing, slowing, and advective heat loss. This self-destructive feedback gradually closes off narrow fissure sections, although dikes may fail to close completely when cooling at the thin edges is combined with inelastic deformation (Daniels and others, 2012). If the magma pressure driving the eruption remains fixed, increased flow rate in the open sections can widen dikes by melting the layer of congealed magma formed earlier at the wall (Bruce and Huppert, 1989, 1990). Attainment of a stable fissure width reflects thermal equilibrium between conducted, radiative, and advective heat. The duration of flow is then controlled by magma pressure. A particularly well documented field example is afforded by the shutdown of the Kupaianaha vent at Kīlauea after nearly 6 years of quasi-steady magma flow. Here, the temperature of erupted lava was constantly 1,152±3 °C over a 10-month period in which magma supply dropped linearly with time from 2.5×10^5 to 5.4×10^4 m^3/d. The linear decay allowed accurate prediction of vent closure and supported a cessation model based on pressure loss rather than cooling (Kauahikaua and others, 1996).

Magma Degassing

> All . . . workers agree that rising gas achieves the work known at the surface of the earth as volcanic activity.
>
> —*Thomas A. Jaggar, Jr.* (1917)

That gas is a driving force for subaerial volcanic eruptions was well known to early 20th century volcanologists (fig. 5*A*; Hitchcock, 1911; Day and Shepherd, 1913; Perret, 1913b; Jaggar, 1917). Gas played a central role in the vivid accounts of Halemaʻumaʻu pyrotechnics from 1907 to 1924, but the origin and constitution of the gas were unresolved, fueling nearly a half-century of vigorous debate. Resolution of contentious issues was beyond reach until methods of measuring gas species and fluxes were improved, and the concept of thermodynamic equilibrium of volatile species was adopted. Studies of the physics of gas exsolution and transport have lagged behind geochemical inquiries, awaiting better constraints on melt viscosity, melt-vapor surface tension, and volatile diffusivity. As experimental data on the relevant physical properties amassed, investigation of the kinetics and mechanisms of phase transformation commenced through application of classical nucleation theory and quantitative textural analysis of pyroclasts. Adaptations of engineering models for two-phase flow (bubble and melt) fueled quantitative analysis of how gas propels and fragments magma during the final stages of ascent.

Geochemistry of Degassing

From the early days of HVO, Halemaʻumaʻu lava lake provided scientists with direct access to volcanic gases (see Sutton and Elias, this volume, chap. 7). Gas samples collected between 1912 and 1919 established carbon and sulfur as important components in volcanic gas, but the role and origin of water in Hawaiian eruptions remained an enigma. Some workers proposed that percolating meteoric water (or seawater) was ingested by magma at depth (Green, 1887; Dana, 1890; Brun, 1911). In opposition, Day and Shepherd (1913) argued that "[water] is entitled to be considered an original component of the lava with as much right as the sulphur or the carbon," whereas Jaggar (1917) stated unequivocally that gases other than water (sulfur and carbon) "operate the volcanic engine."

As time went on, earlier maxims were shed. Shepherd (1938) discounted his early work on Halemaʻumaʻu gas samples, lamenting the impossibility of determining original compositions and concentrations of juvenile magmatic gas from the types of samples that were collected. By that time, he recognized that the gas samples were invariably contaminated by atmospheric and organic components, regardless of the volcanic setting or the collection methods used. After reevaluating data from samples collected in 1917–19, Jaggar (1940) also reversed his original assertion and conceded that H_2 is a primal magmatic volatile, although he remained convinced that molecular H_2O is not primary.

Progress on gas geochemistry stalled until midcentury, when Ellis (1957) showed that "modern" chemical thermodynamics could be used to establish relevant volatile equilibria. Moreover, he demonstrated that balanced reactions could be used to deduce the primary volatile species in samples at conditions other than those of collection, thus providing a means to correct for unavoidable atmospheric and organic contamination. His work stimulated a flurry of studies that used a thermodynamic-equilibrium approach, firmly establishing C-O-H-S as the primal volatile species dissolved in Hawaiian basaltic magma (Matsuo, 1962; Heald, 1963; Finlayson and others, 1968; Gerlach and Nordlie, 1975a-c; Volkov and Ruzaykin, 1975). Thermodynamic calculations were facilitated by increasing use of digital computers (Heald and Naughton, 1962) and new sampling techniques (for example, Naughton and others, 1963, 1969; Giggenbach 1975; see Sutton and Elias, this volume, chap. 7).

A critical link between gas thermodynamics and eruption dynamics was forged in papers that placed C-O-H-S geochemical studies in the context of the geometry of Kīlauea's plumbing system and magma-supply rates (fig. 5*B*; Gerlach and Graber, 1985; Greenland and others, 1985; Gerlach, 1986; Gerlach and others, 2002). These papers demonstrated that at mantle levels, ~0.3 weight percent H_2O, 0.7 weight percent CO_2, and 0.1 weight percent S are dissolved in primary Kīlauea magma. About 90 weight percent of the CO_2 exsolves during ascent to the base of the summit reservoir at ~7 km (180 MPa lithostatic pressure, 4 volume percent gas). The newly arrived magma is strongly buoyant, relative to the resident magma, and should rise from the point of entry as a turbulent plume that mixes thoroughly and equilibrates to chamber conditions (75–180 MPa; Gerlach and others, 2002). In recent times, CO_2-rich gases are emitted passively from the summit reservoir at a rate of 9,000–25,000 metric tons per day (Gerlach and others, 2002; Poland and others, 2012; see Sutton and Elias, this volume, chap. 7). Reservoir-equilibrated magma contains dissolved volatile concentrations of ~0.3 weight percent H_2O, ~0.1 weight percent S, and from 0.02 to 0.1 weight percent CO_2, depending on the depth of equilibration (Greenland and others, 1985; Gerlach and others, 2002). These residual volatiles exsolve at very low pressures (<10 MPa) as the reservoir-equilibrated magma approaches the surface during eruptions.

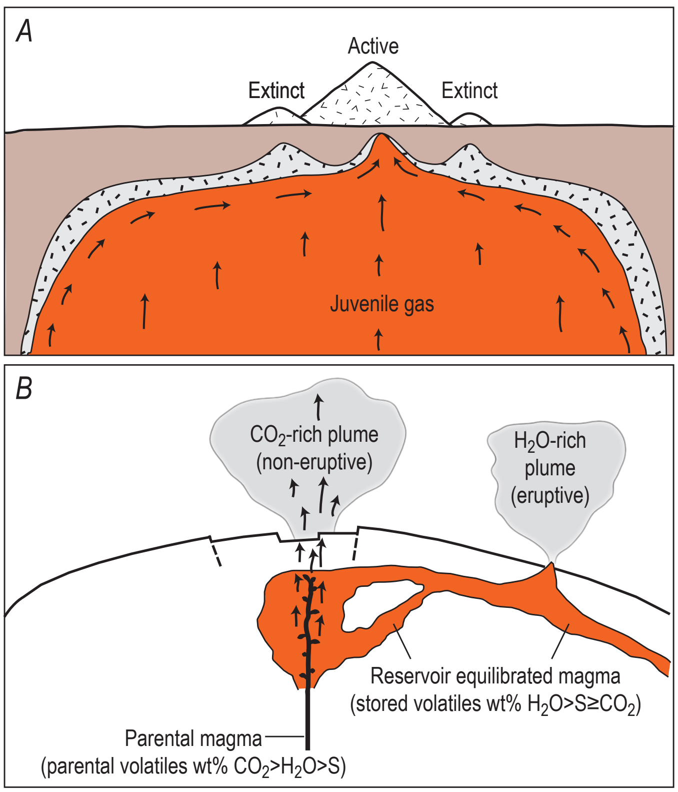

Figure 5. Conceptualizations of magmatic degassing, then (*A*) and now (*B*). *A*, A visit to Kīlauea in 1909 led R.A. Daly to postulate that buoyancy-driven flow of C-N-Cl-S-H juvenile “fluid” to highest point in “feeding chamber” dictated position of eruption sites. Neighboring vents, robbed of juvenile gas by “the advantage of the middle vent,” are extinct. Daly reasoned that gas exsolution commenced at depths of several kilometers, while admitting that it was an assumption “necessarily difficult to test by the facts of field geology.” Modified from Daly (1911). *B*, Better understanding of Kīlauea’s plumbing system and, in 1980, start of systematic gas monitoring by the Hawaiian Volcano Observatory made a critical link between the geochemistry and depth of magma degassing and the dynamics of eruptions. Sketch shows passive CO_2-rich degassing of parental magma at level of summit reservoir and shallow degassing of H_2O-rich volatiles during rift-zone eruptions. Modified from Gerlach and Graber (1985).

Physics of Gas Bubbles

In comparison with the geochemistry of gas, the physics of vesiculation and its bearing on eruption processes received little quantitative attention until the second half of the 20th century because data constraining the physical properties of basaltic melt were few. Recognizing the importance of quantitative physical characterization of magma, Macdonald (1963) compiled existing early measurements of temperature, bulk viscosity, dissolved-gas content, and melt density of erupting Hawaiian basalt. In the 1970s and 1980s, the application of analytical equipment capable of high-resolution, direct measurements provided additional data, including the poorly known, but essential, properties of melt-vapor surface tension and volatile diffusivity (for example, Bottinga and Weill, 1972; Shaw, 1972; Murase and McBirney, 1973; Khitarov and others, 1979; Watson and others, 1982; Zhang and Stolper, 1991).

Kinetics of Bubble Nucleation and Growth

A pivotal paper by Sparks (1978) provided an early, physics-based model for the kinetics of bubble growth during magma ascent. The crux of his paper is a numerical model for diffusional and decompressional bubble growth under various magma-ascent rates, melt viscosities, and H_2O concentrations, solubilities, and diffusivities. Diffusive growth, modeled as $r \propto B(Dt)^{-1/2}$ (Scriven, 1959), where r is the bubble radius, B is the rate constant, D is the volatile diffusivity, and t is the growth time, was shown to be important in the early stages of magma ascent but to trail off with the dwindling reserve of dissolved volatiles. Higher diffusivity leads to more rapid bubble growth. For a given diffusivity, instantaneous growth rates rise with increasing supersaturation because B is large in supersaturated melts. At first, this result may appear counterintuitive, but B is independent of D and is related only to the “yield” of volatile molecules vaporizing at the gas-melt interface. Interestingly, B buffers the kinetics of phase growth in Sparks’ model so that, all other things being equal, the final bubble size (and time-averaged growth rate) is independent of initial supersaturation. Decompressional growth—the simple expansion of a bubble due to a pressure drop—was determined to be most important in the later stages of magma ascent, with bubble size modeled as $r \propto (P_o/P)^{1/3}$ over decompression from pressure P_o to P.

The first comprehensive models for bubble nucleation in basaltic melts came a decade later, most notably in two papers by Bottinga and Javoy for submarine eruption of mid-ocean-ridge basalt (1990) and for subaerial eruption of Kilauean tholeiite (1991). Their work applied classical nucleation theory (for example, Frenkel, 1955), in which the free energy of formation ($\Delta G(i)$) of a bubble nucleus from a cluster containing i volatile molecules is given by the relation

$$\Delta G(i) = RT\ln(C_n/C_e) + A(i)\sigma, \quad (1)$$

where R is the gas constant, T is the temperature, $A(i)$ is the surface area of a bubble nucleus at the pressure of interest, σ is the surface tension, and C_n/C_e is the supersaturation ratio, where C_n is the concentration of dissolved volatiles at the onset of nucleation and C_e is the equilibrium concentration at ambient pressure. Creation of a stable bubble nucleus ($\Delta G(i)<0$) requires a level of supersaturation sufficient to offset the energy required to form a bubble wall. Consequently, higher degrees of supersaturation are needed at low pressure because of the larger surface area of incipient bubbles. In contrast to early degassing models, wherein nucleation was assumed to occur at small supersaturation (Sparks, 1978; Wilson and Head, 1981; Gerlach, 1986), the analysis by Bottinga and Javoy (1991) predicted significant "bubble-nucleation difficulties at low pressure," requiring $C_n/C_e \geq 3$ to trigger nucleation of H_2O or CO_2 bubbles at pressures below 20 MPa (or a depth of <800 m, assuming a lithostatic pressure gradient). Once triggered, however, nucleation is rapid because of high supersaturation, with the nucleation rate, J, proportional to $t^{-1}\exp(C_n/C_e)$, where t is the time needed to accrete a stable nucleus from collisions of randomly fluctuating volatile molecules.

In tandem with theoretical investigations, researchers were exploring the use of bubble-size distributions for empirical derivations of bubble nucleation and growth kinetics (for example, Toramaru, 1989, 1990; Sarda and Graham, 1990). Our own papers (Mangan and others, 1993; Cashman and Mangan, 1994; Mangan and Cashman, 1996) specifically addressed shallow, H_2O-rich degassing during subaerial eruptions along Kīlauea's East Rift Zone. We adapted methods from studies of magmatic crystallization (Cashman and Marsh, 1988), with bubble-size measurements from rapidly quenched pyroclasts plotted as cumulative number distributions. On log-linear plots, the intercept at "size zero" gives the number density of bubble nuclei, and the slope determines the dominant bubble size of the population. If the time scale of vesiculation is known, time-averaged bubble nucleation and growth rates can be calculated directly from the intercept and slope, respectively.

Using measured magma-ascent rates to infer vesiculation time scales, we determined that bubble-growth rates of $\sim 10^{-4}$ cm/s characterize a wide range of eruption intensities, from low-level effusion (mass eruption rates of $\sim 10^3$ kg/s) to high-energy lava fountaining (mass eruption rates of $\sim 10^5$–10^6 kg/s), with a dominant bubble size for both populations of ~ 0.01 cm. That time-averaged (not to be confused with instantaneous) bubble-growth rates and final bubble size are similar across the energy spectrum is consistent with the modulating effects of the rate constant B (Sparks, 1978). Nucleation rates, in contrast, increased by several orders of magnitude as a function of mass eruption rate: rates of ~10 events/cm^3 per second were calculated for low-energy effusive eruptions, whereas rates of $\sim 10^4$ events/cm^3 per second were obtained for high-energy lava fountains. Such extreme nucleation rates imply an intense vesiculation burst at high degrees of volatile supersaturation.

Collectively, the theoretical and empirical results summarized above highlight a largely overlooked conclusion by Verhoogen (1951, p. 729) about the controls on explosive volcanism:

> The most important single factor appears to be the number of bubbles which form per unit volume of time. The problem is similar to that of nucleation of crystals; and it is argued that differences in behavior of erupting volcanoes may depend more on the kinetics of the processes involved than on original differences in composition, gas content, depth, etc.

A plot of bubble number densities (a proxy for nucleation rate) of pyroclasts from several Hawaiian-style eruptions as a function of mass eruption rate (fig. 6) illustrates the truth of Verhoogen's statement.

Bubble Interactions

As the percentage of gas increases, the physics of bubble interactions becomes important. Chemical engineering studies on the behavior of polymer bubble suspensions (<74 percent porosity) and foams (≥74 percent porosity) suggest that bubbles begin to "feel" the effects of their neighbors when their separation distances are nearly equivalent to their radius (Ivanov and Dimitrov, 1988). In a homogenous distribution of similar-size bubbles, geometric considerations give the nearest-neighbor distance as bubble number density to the -⅓ power (Underwood, 1970). Bubble number densities characteristic of basaltic eruptions (10^2–10^7/cm^3) suggest that interactions between bubbles as small as 10^{-3} to 10^{-1} cm cannot be neglected.

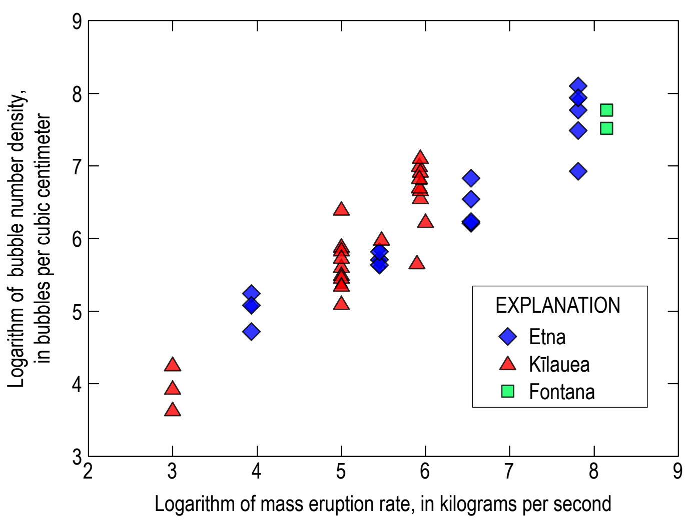

Figure 6. Plot of bubble number densities (BND) of rapidly quenched pyroclasts from Hawaiian-style eruptions, showing a positive correlation with mass eruption rates (MER), according to the expression log(BND)=0.73log(MER)+1.98 (correlation coefficient r^2=0.85). Hawai'i BNDs from Mangan and others (1993), Mangan and Cashman (1996), Stovall and others (2011, 2012), and Parcheta and others (2013), with MER calculated from data of Richter and Murata (1966), Swanson and others (1979), Heliker and others (2003), assuming a density of basaltic melt of 2,600 kg/m^3; Etna data from Polacci and others (2006), Sable and others (2006), and Rust and Cashman (2011); Fontana data from Costantini and others (2009, 2010).

Of considerable relevance in basaltic systems is the physics of bubble coalescence, expansion, and ripening. Expansion dominates as bubbly melt approaches the Earth's surface because of the large increase in gas volume at low pressure. At a fixed gas volume, both coalescence and ripening (redistribution of gas from small to large bubbles) increase the characteristic bubble size and decrease the bubble number density. Understanding the processes that change how a specific volume of gas is partitioned in the melt—whether as many tiny bubbles or as few, very large bubbles—bears significantly on the rheology of magma.

Verhoogen's (1951) study is one of the earliest on the physics of coalescence in basaltic bubble suspensions (<74 percent porosity). He reasoned that bubbles rise buoyantly through a column of magma at rates proportional to their size, allowing larger, faster bubbles to overtake, collide with, and "swallow up" smaller, slower bubbles. Later modeling of coalescence in Hawaiian lavas defined a "linear collection efficiency" term given by the radius ratio of small to large bubbles (Sahagian, 1985; Sahagian and others, 1989). If this ratio is very small (large size difference), coalescence is unlikely because larger bubbles are swept past smaller bubbles without collision. Similarly, a ratio near unity (equal sizes) is also unlikely, because there is little chance that one bubble will overtake the other.

In circumstances where bubbles do collide, bubble size continues to be important. At least one of the colliding pair must deform to ingest the other. Small bubbles resist deformation by virtue of surface tension and high internal pressure, as is deducible from the Young-Laplace law, which gives internal bubble pressure (P_{internal}) as a function of surface tension (σ), bubble radius (r), and ambient pressure (P_{external}):

$$P_{\mathrm{internal}} = P_{\mathrm{external}} + \sigma/r. \qquad (2)$$

Theoretical and experimental studies of basaltic systems (melt viscosity, 10–10^3 Pa-s) suggest that bubbles must be at least several millimeters in diameter before the wavelength of a disturbance (collision) creates significant deformation of the bubble wall (Manga and Stone, 1994; Suckale and others, 2010).

The net result of collision-based models is that the smallest bubbles have the lowest probability of coalescing, as demonstrated empirically by the perturbations observed in bubble-size distributions of Kīlauea pyroclasts, which show the signature of bubble coalescence at sizes >0.1 cm (Mangan and others, 1993; Cashman and Mangan, 1994; Mangan and Cashman, 1996; Herd and Pinkerton, 1997; Stovall and others, 2012; Parcheta and others, 2013) and in experimental studies using analog fluids (for example, Pioli and others, 2012).

In magmatic foams (≥74 percent porosity), bubble coalescence hinges on interstitial melt flow and typically involves ingestion of many bubbles simultaneously. Closest packing of uniform-size spherical bubbles (74 percent porosity) or deformed polyhedral bubbles (>74 percent porosity) provides a basic conceptual model for magmatic foams that is consistent with the structures observed in basaltic pyroclasts (Mangan and Cashman, 1996). The areas of contact between bubbles form lamellae, or films. The geometry of packing requires that three films meet at dihedral angles of 120°, which form channels, or plateau borders, that are trigonal in cross section. Four plateau borders intersect at ~109º to form tetrahedral vertices. Also important are geometric constraints on close packing of uniform polyhedra. Dana (1890) first described the geometry of basaltic foams, which he described as "thread-lace scoria" (now known as reticulite with ≥90 percent porosity) that formed in high lava fountains (Mangan and Cashman, 1996). The regularity of the polyhedral cells in these clasts approaches that required by energy minimization (reduction of melt-gas interfacial area to gas volume), as shown by comparison of observed cell shapes with those predicted mathematically by Weaire and Phelan (1994).

Drawing insight from chemical engineering studies (for example, Hass and Johnson, 1967; Ramani and others, 1993; Sonin and others, 1994), models of coalescence in basaltic foams assume that interstitial melt flows from bubble films (film thinning) to plateau borders, which, in turn, drain downward under the influence of gravity (Jaupart and Vergniolle, 1988; Toramaru, 1989; Proussevitch and others, 1993; Mangan and Cashman, 1996). Mangan and Cashman (1996) equated the rate of film thinning, V_{f}, to the driving pressure for flow, ΔP:

$$V_{\mathrm{f}} = \Delta P(\Delta^3/3\eta r_{\mathrm{c}}^2), \qquad (3)$$

where δ is the film thickness, η is the melt viscosity, and r_{c} is the radius of the contact surface between bubbles. The formulation of ΔP may relate to the force of expansion (pressure exerted on melt in the interstices between expanding bubbles), capillary forces (interfacial pressure gradient due to bubble wall curvature), and (or) gravitational forces (downward drainage through melt channels). Measurements on rapidly quenched pyroclasts from Kīlauea eruptions suggest that basaltic melt films may become extremely thin (Δ~10^{-4} cm) before rupture and coalescence occur (Mangan and Cashman, 1996). In engineering applications, bubble-wall thinning and rupture distinguish open-celled (high permeability) from closed-celled (low permeability) foams. In magmatic foams, the degree to which these processes occur, relative to quenching, distinguishes basaltic pumice (quasi-closed cell) from scoria and reticulite (quasi-open cell).

Gas partitioning in basaltic foams is also influenced by Ostwald ripening, a process first described by the German chemist Wilhelm Ostwald in 1896. Ripening involves diffusive transfer of gas from small to large bubbles due to pressure excess inside bubbles, which, from the Young-Laplace law, is high for small bubbles and low for large bubbles. Since bubbles in magmatic foams vary in size, gas will diffuse across bubble films from regions of high to low pressure. Large bubbles will grow, while small bubbles will shrink. Mangan and Cashman (1996) borrowed an expression for ripening time, t, from de Vries (1972), in which bubble size changes as

$$\Delta r = t(4RTDC_{\mathrm{e}}\sigma/\Delta P\delta), \qquad (4)$$

where R is the gas constant, T is the temperature, D is the diffusivity, C_e is the equilibrium dissolved-gas concentration, σ is the surface tension, P is the external pressure, and Δ is the film thickness. Results indicate that basaltic foams can ripen significantly over time scales of a few tens of seconds at $\Delta \leq 0.005$ cm. Even at porosities as low as 10–20 percent ($\Delta \sim 0.01$ cm), experimental studies have shown that significant ripening occurs, albeit on time scales of hours to tens of hours (Lautze and others, 2011).

Effect of Gas Partitioning on Magma Viscosity and Magma Flow Regimes

Attempts to determine the viscosity of molten basalt date back to the late 1800s and early 1900s in Hawai‘i, with hydrodynamic measurements in lava channels and lava lakes (for example, Becker, 1897; Palmer, 1927; Kinsley, 1931; Macdonald, 1954, 1955; Shaw and others, 1968). Most influential were the rotational viscometry measurements by Shaw and others (1968) in the 1965 Makaopuhi lava lake on Kīlauea's East Rift Zone (Wright and Okumura, 1977). Combining the lava-lake data with those from laboratory experiments using bubbly silicon oils, Shaw (1972) was one of the first to recognize that bubbles variously influence magma viscosity. He observed a viscosity increase at low shear but a viscosity decrease at high shear that he attributed to bubble deformation (Shaw and others, 1968, p. 252):

> This behavior at high shear rates appears to be related to the distortion of the bubbles, which become drawn out into annular zones effectively decreasing the shear resistance. The cause of stiffness at low shear rates is complex, but qualitatively the surface tension of the bubbles opposes distortion.

The effect of bubble size on viscosity was also recognized by Shimozuru (1978), who contrasted the behavior of large, deforming bubbles with that of small, spherical bubbles that act as rigid "obstacles" to increase shear viscosity. With insight from Hawaiian lava lakes, Shimozuru was also one of the first researchers to conceptualize the rheology of bubble+melt mixtures rising in eruptive conduits using engineering terms, specifying bubbly or slug flow regimes, depending on bubble size. The application of two-phase flow mechanics has since become entrenched in volcanology.

Bubbles and Viscosity

Many theoretical and laboratory studies followed Shaw's (1972) pivotal viscosity experiments in Makaopuhi lava lake (for example, Stein and Spera, 1992; Crisp and others, 1994; Manga and others 1998; Spera, 2000; Manga and Loewenberg, 2001; Rust and Manga, 2002; Pal, 2003; Llewellin and Manga, 2005; Harris and Allen, 2008). Crystals are well known to increase the shear viscosity of a magma+crystal suspension by an amount,

$$\eta\left(1-\frac{\phi}{\phi_c}\right)^{-\phi_c}, \tag{5}$$

where η is the melt viscosity, ϕ is the volume fraction of crystals, and ϕ_c is the volume fraction of crystals at maximum packing. For the near-liquidus, low-crystallinity magmas of most Hawaiian-style eruptions, however, the shear viscosity of a melt+crystal suspension is less than a factor of 2 above that of the melt phase alone (1,200–1,150 °C and ≤20 percent crystallinity).

The impact of bubbles on shear viscosity, in contrast, is a complex interplay between bubble deformation, magma shear rate, and porosity (Manga and others, 1998; Manga and Loewenberg, 2001; Pal, 2003; Llewellin and Manga, 2005). A single dimensionless number—the capillary number, defined as

$$Ca = \eta\gamma r/\sigma, \tag{6}$$

where η is the melt viscosity, γ is the shear rate, r is the bubble radius, and σ is the surface tension—represents the balance between two opposing forces: shear stress promoting bubble deformation and surface tension resisting bubble deformation (fig. 7). Pal (2003) showed that for Ca<<1, spherical bubbles have the same effect as rigid particles and increase shear viscosity, with the viscosity of the suspension, η_s, given by

$$\eta_s = \eta\left(1-\frac{\phi}{\phi_m}\right)^{-\phi_m}, \tag{7}$$

where ϕ is the bubble volume fraction and ϕ_m is the volume fraction of spherical bubbles at maximum packing (~0.64 for bubbles of uniform size). For Ca>>1, deformed bubbles aligned in the direction of flow reduce the shear viscosity, with

$$\eta_s = \eta\left(1-\frac{\phi}{\phi_m}\right)^{1.67\phi_m}. \tag{8}$$

Melt viscosity does not vary widely across the spectrum of Hawaiian-style eruptions, and so the product γr is a key determinant of Ca.

Bubbles and Flow Regimes

Four two-phase flow regimes are generally used to describe the flow of magma-gas suspensions in eruptive conduits: bubbly flows, containing discrete, small gas bubbles; slug flows, in which large pockets of gas rise through the magma; annular flows, comprising a central gas jet sheathed in a coherent melt layer flowing along walls of the conduit; and dispersed flows, in which gas carries suspended melt droplets (fig. 8; see reviews by Jaupart, 2000, Houghton and Gonnerman, 2008). The behavior of bubbly flows is strongly controlled by buoyant and viscous forces. Laminar flow conditions are a good approximation, with the rate of flow decreasing near the conduit walls, owing to viscous drag (wall friction) and increasing inward to the medial axis. At the other end of the spectrum are dispersed flows, which are largely controlled by gas expansion and inertial forces, owing to the low viscosity of gas. Dispersed flows are turbulent,

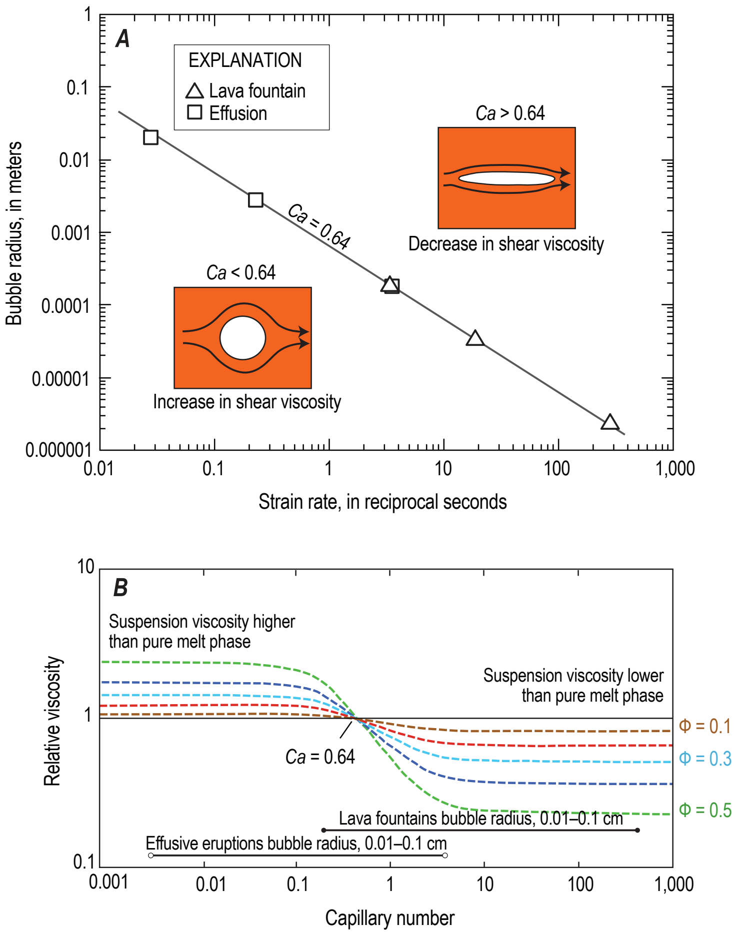

Figure 7. Graphs illustrating how bubbles influence shear viscosity of basaltic magma during Hawaiian-style eruptions. *A*, Bubble radius (*r*) versus strain rate (γ) for which capillary number (*Ca*)=0.64. To right of $Ca_{0.64}$ curve, shear viscosity decreases because of bubble deformation; left of the $Ca_{0.64}$ curve, shear viscosity increases because bubbles, acting as rigid particles, resist deformation. Calculations assume a melt viscosity of 100 Pa-s and a melt-vapor surface tension of 0.1 J/m^2 (Khirtov and others, 1979) for hydrous basaltic melt. Strain-rate estimates for low-energy effusive eruptions and high-energy lava fountains were calculated by using γ=2*u*/3*R*, where *u* is average flow velocity in a vertical, cylindrical conduit of radius *R* (for example, Mastin and Ghiorso, 2000). A range of strain rates was examined, assuming conduit radii of 0.5 to 2.5 m and flow velocities of 0.1 to 320 m/s, which were derived from eruptive fluxes reported for Puʻu ʻŌʻō lava fountaining (Heliker and Mattox, 2003, table 1, episodes 20–39) and Kupaianaha effusive activity (1991 very low frequency [VLF] determinations in Sutton and others, 2003, table 1). *B*, Effect of porosity (Φ) on relative shear viscosity of basaltic magma (viscosity ratio of melt+bubbles/pure melt). For *Ca*>0.64, bubbles decrease shear viscosity of bubble-melt suspensions, relative to that of pure melt; for *Ca*<0.64, bubbles increase shear viscosity. Plot is modified from Pal (2003) for conditions relevant to Hawaiian-style eruptions. Black solid lines span capillary numbers for bubbly conduit flow, terminated by open circles (effusive eruptions) and filled circles (lava fountains). Strain rates were estimated, as in figure 7*A* (effusive eruptions γ~0.03-3.0 s^{-1}; lava fountains γ~2-425 s^{-1}, assuming conduit radii of 0.5–2.5 m).

with a constant mean velocity across the width of conduit, owing to low wall friction.

Between these two end members, flow behavior is complex, because buoyant, expansive, viscous, and inertial forces are all-important. In slug flows, melt moves around the slug at a rate controlled by viscous forces at the wall, rather than by interfacial forces at the melt-slug boundary. Mixed viscous and inertial forces complicate the ascent of the gas slug, with differential gas expansion causing the slug nose to accelerate, relative to the slug base (James and others, 2008). A melt layer along the conduit walls is characteristic of annular flows, with the direction of flow either concurrent or countercurrent to the flow of gas, depending on the velocity of the gas phase and the viscosity of the liquid. Interfacial forces at the gas-melt boundary are consequential in this regime, creating instabilities in the melt film (waves) and making the melt rheology (laminar versus turbulent, steady versus unsteady) exceedingly difficult to ascribe. Melt droplets detach from unstable regions and become entrained in the gas phase. At a high proportion of droplets, the flow becomes dispersed. Bubbly flows and slug flows also transition into dispersed flows upon fragmentation.

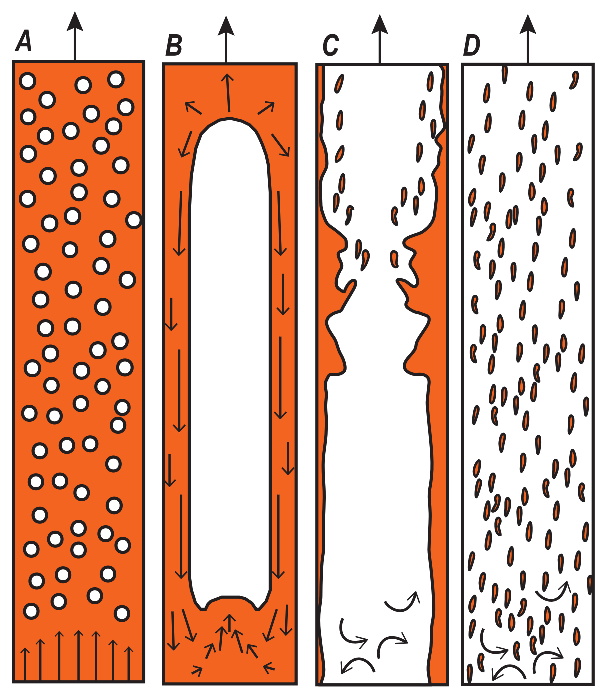

Figure 8. Diagram showing two-phase flow regimes proposed for mixtures of gas and low-viscosity silicate melt rising in a vertical conduit during Hawaiian-style eruptions. Black arrows within red fields (melt) indicate laminar flow of melt, with arrow length indicating relative velocities; black curved arrows in white fields (gas) indicate turbulent flow of a continuous gas phase. In natural volcanic systems, bubbly flows (*A*) may transition to slug flows (*B*) by way of bubble coalescence, or to dispersed flow (*D*) by way of fragmentation. Lava fountains have characteristics of dispersed flows. Annular flows (*C*) are attributed to large-scale, violent foam collapse. Shredding of bounding melt sheath may cause transition from annular to dispersed flows.

Fragmentation of Gas-Charged Magma

Verhoogen (1951) was the first researcher to apply classical hydrodynamics to the fragmentation of basaltic magma, arguing that fragmentation results from violent "coalescence of a large number of bubbles expanding radially faster than they can rise and escape at the surface. . . ." Later, McBirney (1963), McBirney and Murase (1970), and Sparks (1978) argued that coalescence-driven fragmentation is controlled by the geometric limits to bubble packing, which was assumed to be ~75 percent by analogy to maximum packing of uniform-size rigid spheres. Later, Mangan and Cashman (1996) pointed out that high vesicularity does not necessarily lead to fragmentation of bubbly flows, because some effusively erupted basalts have porosities of >75 percent.

More recent experiments and theoretical treatments show that rapidly accelerating, low-viscosity magma may undergo shear-induced liquid breakup irrespective of a critical porosity (Mader and others, 1997; Papale and others, 1998; Cashman and others, 2000; Namiki and Manga, 2008; Rust and Cashman, 2011). The experimental results of Namiki and Manga (2008) emphasize that fragmentation of vesiculating low-viscosity basaltic magma fundamentally differs from that of more viscous, silicic magma. In basaltic systems, inertial forces stretch and "pull apart" rapidly rising, expanding magma. Silicic fragmentation, in contrast, is characterized by brittle failure at high tensile stress. Mangan and Cashman (1996) argued qualitatively that an intense burst of bubble nucleation and growth at high volatile supersaturation could cause the accelerations and shear rates leading to liquid breakup during Hawaiian lava fountaining. Rust and Cashman (2011) have since found evidence for liquid breakup in basaltic lava fountains in the poor correlation between bubble size and pyroclast size. In Strombolian-style eruptions, which have been interpreted as reflecting breakage of individual large bubbles in the slug flow regime, liquid breakup is controlled by the near-surface dynamics (James and others, 2008). As the vent is approached, the nose of the slug is expanding rapidly, relative to the slug base. The lag in momentum causes the slug base to rebound, inducing an upward-directed pressure transient that causes bursting at the nose.

Post-Fragmentation Evolution of Molten Pyroclasts

The physical evolution of a bubbly magma does not stop at fragmentation. Pyroclasts continue to expand in the conduit and fountain as they adjust to ambient pressure, and they may continue to do so upon deposition until the glass transition temperature is reached. Post-fragmentation coalescence and ripening also increase the mean bubble size and reduce the bubble number density. In their treatise on the features of basaltic rocks, Wentworth and Macdonald (1953) alluded to the continuous evolutionary nature of molten pyroclasts in their statement "In a genetic series reticulite lies between pumice and ash." The evolution of magmatic foams is plotted in figure 9. Bubble expansion, coalescence, deformation, and ripening transform a suspension of multisize spherical bubbles into a polygonal foam with a preponderance of pentagonal and hexagonal faces, increasing bubble size by an order of magnitude (from 0.01 to 0.10 cm), decreasing the bubble number density by three orders of magnitude (from 10^5 to 10^2 cm^{-3}), and reducing the interfacial surface area per unit volume of melt by ~75 percent (55 to 13 cm^{-1}).

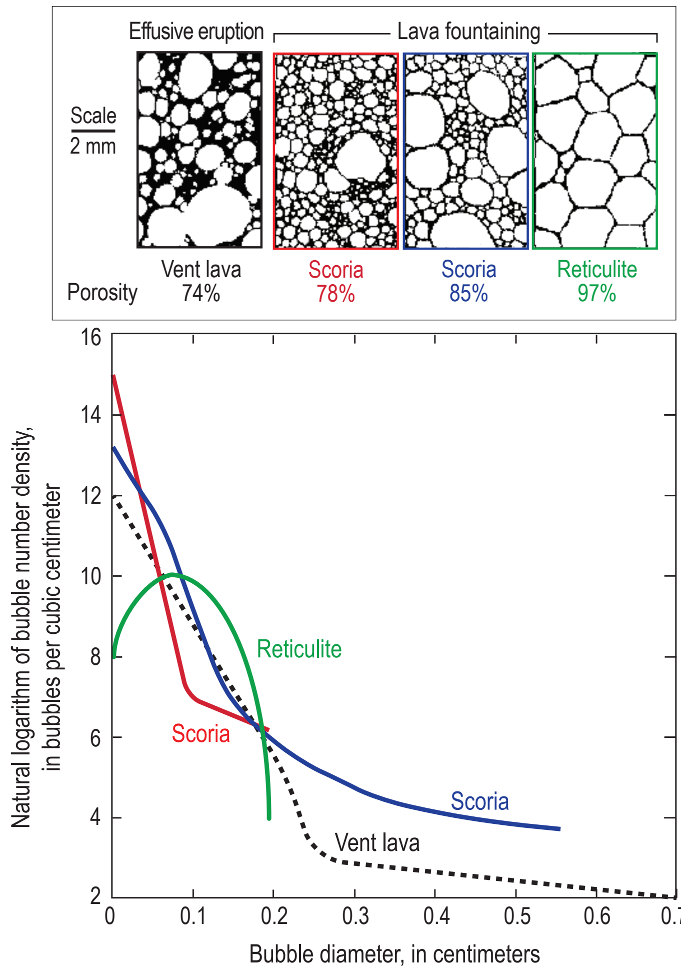

Figure 9. Graph of natural logarithm of cumulative bubble number density as a function of bubble diameter for Kīlauea lava fountain pyroclasts and effusively erupted lava, with binary thin-section images of samples. On such plots, log-linear distributions are expected only for steady-state bubble nucleation and growth due to volatile exsolution and decompressional expansion. Data distribution is distorted from log linearity by coalescence (deflection upward at large size fractions; scoria and effusive lava) and ripening (concave downward; reticulite). Thin-section images illustrate continuous structural evolution from spherical foam (≥74 percent porosity) to polyhedral foam (>97 percent porosity). See Mangan and Cashman (1996) for details.

The preserved porosities of fountain pyroclasts reflect a competition between post-fragmentation expansion, permeability increase (interconnected bubbles), and outgassing (gas flowing out of the pyroclast; not to be confused with degassing, which involves volatile exsolution from melt into bubbles). Rust and Cashman (2011) demonstrated that the permeability of mafic pyroclasts increases by two orders of magnitude as porosity rises from 45 to 70 percent. They suggested that once pyroclasts begin to outgas, further expansion is limited, "much like a hole in a balloon can make it impossible to further inflate." Expansion dominates over outgassing for $k/R^2<\eta_{gas}/\eta_{melt}$, where R is the pyroclast radius (length scale for gas flow), k is the pyroclast permeability, η_{gas} is the viscosity of the gas, and η_{melt} is the viscosity of the melt (fig. 10). In contrast to silicic pyroclasts, the low viscosity of near-liquidus basalt and the coarseness of fountain ejecta favor significant expansion. In further contrast, a condition of dynamic permeability exists in low-viscosity magma that is unlikely to exist at higher viscosity—that is, transient apertures open gas channels between bubbles, only to close again once the gas is released from the pyroclast and the fluid melt relaxes. Because of their fluidity, basaltic pyroclasts may oscillate across the boundary between outgassing- and expansion-dominated behaviors. Sporadic gas loss through dynamic permeability, which is basically gas-melt decoupling on short length and time scales (see subsection below entitled "Models Framed by H_2O-Rich Degassing in the Conduit"), may explain the relatively wide range of vesicularities (Houghton and Wilson, 1989) and the regularity of bubble shapes (Moitra and others, 2013; Parcheta and others, 2013) that distinguish fountain pyroclasts from their more viscous counterparts.

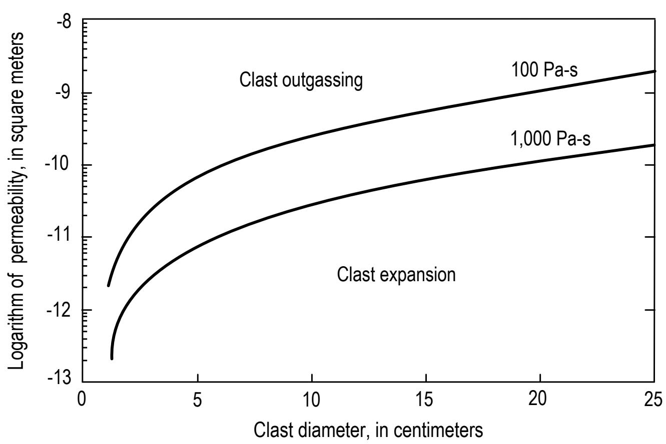

Figure 10. Plot showing conditions for pyroclast outgassing (field above each curve) versus pyroclast expansion (field below each curve), calculated for melt viscosities (η_{melt}) of 100 and 1,000 Pa-s. Curves obtained from relation $k/R^2=\eta_{gas}/\eta_{melt}$. Outgassing is favored by high permeability (k), low melt viscosity, and small pyroclast size (R). Calculations assume gas viscosity (η_{gas}) of 10^{-5} Pa-s. Modified from Rust and Cashman (2011).

Numerical Modeling of Hawaiian-Style Eruptions

The Observatory will measure everything for a century to come.

—*Thomas A. Jaggar, Jr.* (1945)

For uniform conduit geometry, four intertwined and changing parameters influence eruptive behavior: driving pressure, melt viscosity, crystal content, and gas content. This interrelation is seen most simply in the proportionality $Q \propto \Delta P/\eta_f$, where Q is the mass flux, η_f is the bulk magma viscosity (melt+crystals+bubbles), and ΔP is the pressure driving the flow (buoyancy+reservoir overpressure–weight of the overlying magma column). In nature, though, conduits narrow, kink, or flare; reservoir overpressure waxes and wanes; and degassing with or without crystallization causes changes in magma viscosity, buoyancy, and mass. In light of these complexities, Jaggar's call for the observatory to "measure everything" shows much foresight. Direct field measurements are essential to choosing appropriate model input, constraining boundary conditions, and evaluating model results. Not coincidentally, the first numerical models of basaltic eruption dynamics drew heavily from the data archives of the Hawaiian Volcano Observatory.

Overview of Existing Eruption Models

The first computer-assisted numerical models of Hawaiian-style eruptions employing classical conservation equations for mass, momentum, and energy were introduced in the 1980s. The earliest lava-fountain model, constructed by Wilson and Head (1981), considers magma ascending and degassing as bubbly flows (fig. 8*A*), with a transition to dispersed flows (fig. 8*D*) once the porosity reaches 75 percent. Shallow, H_2O-rich degassing is the driver in this model. CO_2, which is both less abundant and less soluble, is assumed to have exsolved and escaped from the system at great depth (see for example, Gerlach and Graber, 1985).

Vergniolle and Jaupart (1986) provided an alternative lava-fountain model, with CO_2-rich degassing as the driving force. In their model, deeply exsolved CO_2 bubbles are not lost to the system; instead, they accumulate as a foam layer at the roof of the subvolcanic reservoir. Lava fountains result from violent annular flows (fig. 8*C*) triggered by spontaneous, wholesale collapse of the foam, once a critical thickness is reached. Secondary H_2O-rich degassing accompanies the depressurization associated with collapse but is assumed to be inconsequential to the physics.

Extensions and refinements to both models, based largely on data and observations from the 1983–86 Puʻu ʻŌʻō fountaining episodes, were presented by Parfitt and Wilson (1994, 1995, 1999), Parfitt and others (1995), Parfitt (2004), Jaupart and Vergniolle (1988), Vergniolle and Jaupart (1990), Vergniolle (1996, 2008), Woods and Cardoso (1997), and Seyfried and

Freundt (2000). These later treatments focused on constructing a continuum model in which transitions between persistent lava-lake activity, low-energy effusive eruptions, and high-energy lava fountains are modulated by styles and rates of gas release.

Models Framed by H_2O-Rich Degassing in the Conduit

The underlying assumption in the H_2O-rich degassing model is that bubble-free magma rises steadily in the conduit until reaching the pressure-depth of H_2O saturation. Bubbles then begin to nucleate and grow by volatile exsolution, decompressional expansion, and, depending on the rise rate of magma, bubble coalescence. Before reaching the saturation depth, magma rise is controlled by reservoir overpressure. Once vesiculation commences, however, the evolution of H_2O-rich gas is what propels magma upward to the surface.

Whether or not the magma is fragmented before reaching the vent depends on how strongly bubbles are coupled to the parcel of melt from which they exsolve. Under Stokes's law, the rise rate of a single bubble is determined by the ratio of bubble buoyancy to viscous drag. At high magma rise rates, bubbles are carried along in the flow, with little independent motion or interaction (limited coalescence or ripening). Wilson and Head (1981) and, later, Parfitt and Wilson (1995) showed that for the melt viscosities,

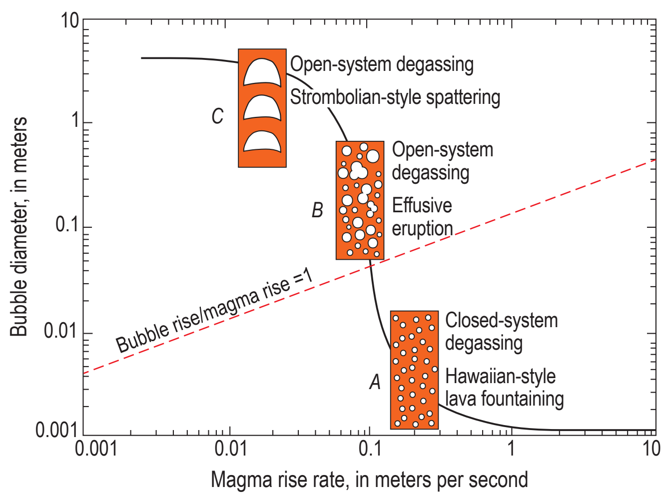

Figure 11. Plot showing curve for maximum bubble diameter achievable as a function of magma rise rate for H_2O-rich degassing during flow in a vertical conduit. Model assumes melt viscosity of 100 Pa-s and initial dissolved H_2O content of 0.5 weight percent. Bubbles are assumed to grow by mass transfer (exsolution), decompressional expansion, and, for magma rise rates <0.1 m/s, coalescence due to bubble collision. For magma rise rates of >0.1 m/s (*A*), Stokes rise rate of bubbles is less than magma rise rate, and closed system degassing leads to lava fountaining (bubbles and melt coupled; no coalescence; not depicted in *A*, bubbly flows transition to dispersed flows near the surface). When Stokes rise rate of bubbles exceeds that of magma (*B*,*C*), open-system degassing leads to effusive eruptions (modest numbers of bubbles coalesce; bubbly flows maintained, *B*) or pulsed, Strombolian-style spattering (significant numbers of bubbles coalesce resulting in slug flow, *C*). Modified from Parfitt and Wilson (1995).

dissolved H_2O contents, and H_2O saturation pressures typical of Hawaiian tholeiite ($10–10^3$ Pa-s, 0.2–0.4 weight percent, and <10 MPa, respectively), magma rise rates of >>0.1 m/s result in strong coupling between bubbles and "parent" melt in the mode of closed-system degassing (fig. 11, location A). The ascending gas-charged magma eventually reaches sufficient porosity (~75 percent) to trigger fragmentation (original model of Wilson and Head, 1981) or, as more recent models convincingly demonstrate, shear-induced liquid breakup (Namiki and Manga, 2008; Rust and Cashman, 2011). The sharp pressure drop and reduced wall friction instigated by fragmentation causes pronounced acceleration of the dispersed flow, which eventually emerges from the vent as a jet of molten pyroclasts and gas. Fountaining ceases when the reservoir pressure returns to a stable state. For quasi-uniform magma supply from depth, waxing and waning reservoir overpressure produces episodic fountains that are regulated by a magmatic "valve" of cooler, high-yield-strength magma that clogs narrow segments of the feeder dike between successive events.

At the other end of the spectrum, magma rise rates of <<0.1 m/s create conditions for open-system degassing with minor eruption of magma (fig. 11*C*). When the magma rise rate is very low, larger bubbles gradually decouple from their parent melt. With differential rise of varying-size bubbles, coalescence can occur. Wilson and Head (1981) suggested that "a runaway situation may eventually develop" in which fast-rising, large bubbles beget faster, larger bubbles until slug flows prevail. Conduit-filling gas slugs burst at the vent, generating Strombolian-style spattering of molten pyroclasts. Slug flows formed by cascading coalescence were observed in large-scale two-phase flow experiments, using analog fluids in a long vertical tube (6.5×0.25 m) scaled to match persistent degassing from a standing column of basaltic magma (Pioli and others, 2012). Though not directly analogous because no bubbles nucleate in the column (gas fluxes from below only), the experiments and related theoretical modeling show that the process of collision-induced coalescence, slug formation, and quasi-steady bursting of slugs at the surface creates circulation cells within the conduit that homogenize and stabilize the magma column. This type of pulsed slug degassing and magma recirculation with negligible discharge of lava is suggested as a plausible mechanism for the rise-fall cycles observed in active Hawaiian lava lakes (Ferrazzini and others, 1991; Parfitt and Wilson, 1994, 2008; Parfitt, 2004; Johnson and others, 2005).

Effusive Hawaiian eruptions lie between the end members above. The continuous extrusion of bubbly lava results from intermediate magma rise rates of ~0.1 m/s (fig. 11, location B). Here, although open-system gas loss occurs because of partial decoupling of bubble and melt, bubbly flow is maintained over the entire length of the conduit. A fraction of larger, coalesced bubbles rising through, rather than with, the magma during effusive eruptions may accumulate as a foam layer at the top of an effusive vent that has skinned over as the result of radiative cooling. Recent field studies at the active Puʻu ʻŌʻō and Halemaʻumaʻu vents demonstrate convincingly that bubbles collecting under a viscoelastic lid at the top of the conduit can lead to sporadic gas-release events and episodic rise-fall cycles without slug flow (Patrick and others, 2011a,b; Orr and Rea, 2012).

Models Framed by CO_2-Rich Degassing in the Subvolcanic Reservoir

Fountaining has been suggested to be triggered by sudden release of CO_2-rich bubbles trapped at a reservoir roof. Here, the roof-conduit connection is assumed to lie at a pressure-depth interval below that of H_2O saturation. The foam layer is generated either internally, by bubbles rising through a static, gas-saturated reservoir, or externally, by quasi-steady supply of bubbly magma to the reservoir from the mantle. With quasi-steady magma supply, magma throughput from reservoir roof to conduit base must be sufficiently impaired by drastic narrowing at the roof-conduit connection, such that bubbles segregate at the roof with only a little magma leaking into the conduit. In either case, an increasing buoyant force is exerted on bubbles pressed against the roof by those arriving from below. Bubbles flatten until the force of surface tension is insufficient to maintain the integrity of bubble walls. The critical thickness, h_c, leading to collapse of the foam layer is modeled as

$$h_c = (2\sigma/\phi_g \rho_m g r), \quad (9)$$

where σ is the surface tension, ϕ_g is the gas-volume fraction in the foam (by definition, ≥ 0.74), ρ_m is the melt density, g is the gravitational constant, and r is the bubble radius (fig. 12). The minimum size of bubbles accumulating at a roof at ambient pressures of ~10 to 100 MPa will range from 0.1 to 1.0 mm in diameter (assuming no coalescence). We derive this constraint from the sizes of CO_2 bubbles measured in basalts erupted along the Mid-Atlantic Ridge (Sarda and Graham, 1990) corrected to the relevant pressure range and from decompression experiments using basalts saturated with mixed H_2O-CO_2 fluids at 400 MPa (Mangan and others, 2006). Thus, as shown in figure 12, the critical thickness of the foam layer ($\phi_g \geq 0.74$) ranges from ~0.1 to 1 m over the spectrum of expected bubble sizes.

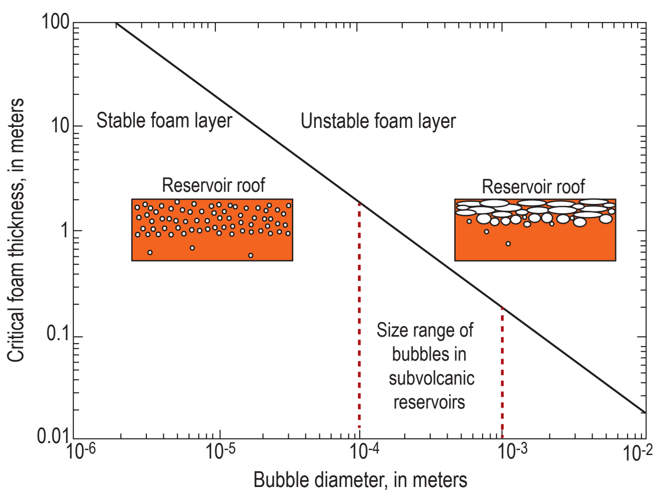

Figure 12. Plot of critical foam thickness versus bubble diameter. Calculation uses formulation of Vergniolle and Jaupart (1990) for critical thickness *(h_c=2σ/$\varphi_g \rho_m g r$)*, with surface tension σ=0.1 kg/s^2, gas fraction of bubbles in foam layer φ_g=0.74, bubble radius *r*, and melt density ρ_m=2,600 kg/m^3. In absence of coalescence, expected size of bubbles at subvolcanic reservoir pressures (0.1–1 mm; ~10 MPa) suggests that foam layers ~1 m thick are unstable. In Hawai‘i, a typical lava-fountaining episode releases ~10^6 m^3 of gas (Greenland, 1988), suggesting unrealistically large reservoir roof areas (~10^6 m^2) for historical eruptions of Kīlauea. We note, however, that formulation for foam stability is consistent with rise-fall cycles documented by Patrick and others (2011b) and Orr and Rea (2012), in which a surface foam layer collapses, releasing 10 to 10^4 m^3 of H_2O-rich gas amid mild spattering.

For a given conduit dimension, the vigor of the ensuing eruptive activity depends on the volume of CO_2 gas spontaneously released by the collapsing foam (given by $h_c S$, where S is the surface area of the roof). If the volume of CO_2-rich gas expelled is large (~10^6 m^3 for lava fountains), the eruption is assumed to be driven by annular flow, with the onset of H_2O-rich degassing only a secondary contribution to upward acceleration. The turbulent core of expanding gas streaming through the conduit shreds the bounding magma layer at the walls to produce the dispersed jet of molten pyroclasts associated with fountaining. Once the volume of trapped foam is expended, fountaining ends. If the flux of bubbles from below is continuous, the cycle begins again with the foam layer building and failing at time scales controlled by the gas-flux rate.

At the other end of the spectrum, effusive eruptions represent circumstances of low gas flux to the roof and (or) a roof-conduit connection that does not appreciably hinder throughput of magma to the conduit. The critical foam thickness is never attained, and a steady stream of bubbly magma is erupted without fragmentation. Transitional between end members are those eruptions driven by buildup and spontaneous collapse of small foam volumes. Slugs of CO_2-rich gas cause activity ranging from passive degassing to mild, Strombolian-style spattering of molten pyroclasts.

Dynamic Considerations for Historical Eruptions Based on Reservoir Geometry and Gas Chemistry

Fundamental to the two lava-fountain models described above are the assumed compositions of the gases (CO_2 versus H_2O) propelling magma to the surface and, as a result, the depth (subvolcanic reservoir versus conduit) at which fragmentation occurs. Gas-emission data (composition and volume) and probable reservoir dimensions for Kīlauea's historical lava fountains fit most neatly into the H_2O bubbly-flow model.

For the Pu‘u ‘Ō‘ō fountaining era, for example, scaling the foam-collapse model to satisfy both measured gas volumes (10^6 m^3 of gas erupted per episode; Greenland, 1988) and surface area of the subvolcanic reservoir roof (~400 m^2; Dvorak and others, 1986; Wilson and Head, 1988; Hoffman and others, 1990) is difficult to reconcile with model predictions of critical foam thickness (fig. 12). On a smaller scale and at a shallower level, however, the critical foam thickness predicted by the model shows parity with field data obtained during recent rise-fall cycles at Puʻu ʻŌʻō, albeit for H_2O-rich foam (Patrick and others, 2011b; Orr and Rea, 2012). Here, measured "roof" (viscoelastic skin of lava at the surface) dimensions and volumes of gas release are consistent with near-surface collapse of a foam layer ~1 m thick (fig. 12).

Also problematic for the CO_2 foam-collapse model are the gas-emission data from Puʻu ʻŌʻō fountaining episodes, which suggest low CO_2 concentrations (CO_2/S = 0.2; Gerlach, 1986; Greenland and others, 1988). We note, however, that CO_2-rich degassing could be important if parental magma bypasses Kīlauea's summit reservoir or shoots through it without substantial residence in the shallow crust. Though not requiring foam collapse, the high-fountaining episodes of the 1959 Kīlauea Iki eruption are candidates for syneruptive mixed H_2O-CO_2 degassing. Seismic, tilt, and petrologic data all suggest that rapidly ascending parental magma bypassed the main summit reservoir, intruding into a small, separate storage compartment north of Halemaʻumaʻu, less than 2 months before the onset of eruption (Wright and Fiske, 1971; Helz, 1987). Helz (1987) observed that "the 1959 lava was hotter and more gas-rich than typical Kilauea summit lava," and although no measurements were made to corroborate gas compositions, the extreme H_2O supersaturation implied by the high bubble number densities in Kīlauea Iki scoria led Stovall and others (2011) to propose that "upward forcing" by expanding, previously exsolved CO_2 bubbles led to extreme acceleration and rampant secondary nucleation of H_2O-rich bubbles.

With application of new field-based spectroscopic techniques, instances of eruptive activity driven by mixed H_2O-CO_2 degassing are being documented in basaltic systems. Open-path Fourier transform infrared spectrometry (OP-FTIR) measurements at the peak of fountaining on Mount Etna (Italy) give CO_2/S ratios of ~10, some 2 to 4 times greater than the time-averaged CO_2/S ratios (Allard and others, 2005). OP-FTIR measurements made during sporadic degassing bursts at Puʻu ʻŌʻō in 2004–05 yield CO_2/S weight fractions of ~18 (Edmonds and Gerlach, 2007), close to an order of magnitude higher than those reported by Greenland (1988) for Puʻu ʻŌʻō fountaining episodes. We therefore conclude that vigorous fountaining episodes at Kīlauea can be driven by a combination of CO_2 and H_2O degassing, although the dynamics of mixed-gas eruptions remains poorly understood.

Eruption-Column Models

The structure of a Hawaiian-style eruption column can be diagrammed dynamically as a lower ballistic region of centimeter- to meter-size molten clots dispersed in a gas jet, with an upper convective plume of gas, fine ash, sulfur particles, and aerosols (Head and Wilson, 1989; Sparks and others, 1997). At Kīlauea, typical high-fountaining episodes emit lava and gas at rates of 10^5–10^6 kg/s and 10^3 kg/s, respectively. The ratio of gas to pyroclast is on the order of 70:1 by volume. Direct observations reveal that molten pyroclasts are concentrated in the hot, central axis of the fountain. The thermal core grades outward to a fiery orange-red region of slightly lower temperature and clot concentration, and then to a sparse black halo of quenched pyroclasts "wafted high into the air by the hot turbulently rising fume cloud" (Richter and others, 1970). The temperatures characteristic of fountains can be estimated from olivine-glass geothermometry. Helz and Hearn (1998) found maximum quenching temperatures of 1,160–1,190 °C across a large sample suite comprising Kīlauea Iki and Puʻu ʻŌʻō fountain pyroclasts, with multiple samples from within single fountaining episodes ranging ± ≤10 °C.

Dynamics of the Ballistic Fountain

Molten clots exit the vent at steep angles and reach a height, h_f, approximated by the ballistic equation of motion

$$h_f = u_c^2/2g, \tag{10}$$

where u_c is the exit velocity of pyroclasts and g is the gravitational acceleration. Early models (for example, Walker and others, 1971; Wilson and Head, 1981; Head and Wilson, 1987) assumed conditions of dynamic equilibrium, with a clot velocity less than the gas velocity given by the quantity

$$u_c = u_g - U, \tag{11}$$

where U is the terminal velocity of the clot and u_g is the velocity of the gas. These equations were combined to use fountain height as an indicator of the amount of dissolved volatiles originally stored in the magma. It was later demonstrated, however, that such calculations can be misleading, because substantial kinetic energy is lost by reentrainment of previously erupted, higher density clots that have fallen from the fountain and pooled around the vent (Parfitt and others, 1995; Wilson and others, 1995). Lava recycling at a central vent diminishes the mean clot velocity, u_f, according to

$$u_f = (u_c M)/(M + M_i), \tag{12}$$

where M is the mass flux of fresh lava from the vent, M_i is the radial inflow of recycled, lower density lava coalesced around the vent, and u_c is, as above, the clot exit velocity under conditions of no reentrainment. The energy loss due to recycling can be substantial; for typical mass eruption rates and dissolved H_2O contents, a 1-m-thick pond will decrease fountain height by as much as 35 percent (Wilson and others, 1995).

Another dynamic complexity influencing fountain height was tackled by Parfitt (1998), Wilson (1999), and Parfitt and Wilson (1999). Whereas earlier models assumed that clots were all of uniform diameter and density, Parfitt and Wilson considered the full range of clots across all sizes (d_c) and densities (ρ_c). Unlike the finer, more uniform pyroclasts ejected in silicic eruptions, Parfitt and Wilson determined that, because they are coarser, most basaltic pyroclasts never reach dynamic equilibrium ($u_c \neq u_g - U$). Also, by assuming dynamic equilibrium, earlier models apportioned too much of the internal energy liberated by gas expansion to the kinetic energy of clots, thus leading to an underdetermination of the gas exit velocity by as much as 300 percent. Accounting for the full clast distribution measured in 1959 Kīlauea Iki deposits by Parfitt (1998), Wilson (1999) calculated pyroclast exit velocities ranging from 80 to 250 m/s and a gas exit velocity of ~500 m/s, contrasting, respectively, with the 100 and 125 m/s he had obtained previously, assuming uniform pyroclasts in dynamic equilibrium with the gas (fig. 13*A*).

The Kīlauea Iki case study also showed that >95 percent of the eruptive mass is contained within the ballistic region of the eruption column, with clasts having $d_c\rho_c \geq 100$ kg/m^2 falling within 200 m of the vent (figs. 13*B*,*C*; Parfitt and Wilson, 1999). Inspection of the data tables of Wilson (1999) suggests that only grains with $d_c\rho_c < 0.5$ kg/m^2 are likely to be coupled to the gas and, thus, carried aloft in the buoyant plume rising above the fountain (for example, $d_c = 0.84$ mm, $\rho_c = 600$ kg/m^3; Wilson, 1999, table 1).

Dynamics of a Buoyant Plume

The convective plume of ash, gas, sulfate particles, and sulfuric acid aerosols that billows above a Hawaiian lava fountain offers a pale comparison to the stratospheric phenomena that are silicic ash columns. Most plumes from Hawaiian-style eruptions do not intrude into the tropopause, regardless of latitude or season. Surprisingly, few data exist on the heights of plumes from basaltic eruptions. The 1984 Mauna Loa eruption was one of the few eruptions for which direct measurements of plume height were made. At 7 km above the vent (11 km absolute altitude), the plume top was well below the tropopause, which was at 18-km altitude at the time of the eruption (Lockwood and others, 1984).

Although basaltic eruptions are certainly hotter than silicic ones, much of the thermal energy needed for plume buoyancy is locked in the large molten clots that fall rapidly out of the fountain. Calculations of the time required for thermal waves to travel from a clot interior to the gas flowing rapidly by it indicate that clots larger than 1 cm across probably have residence times too short for substantial heat loss during their upward trajectory (Sparks and Wilson, 1976; Wilson and others, 1978; Woods and Bursik, 1991).

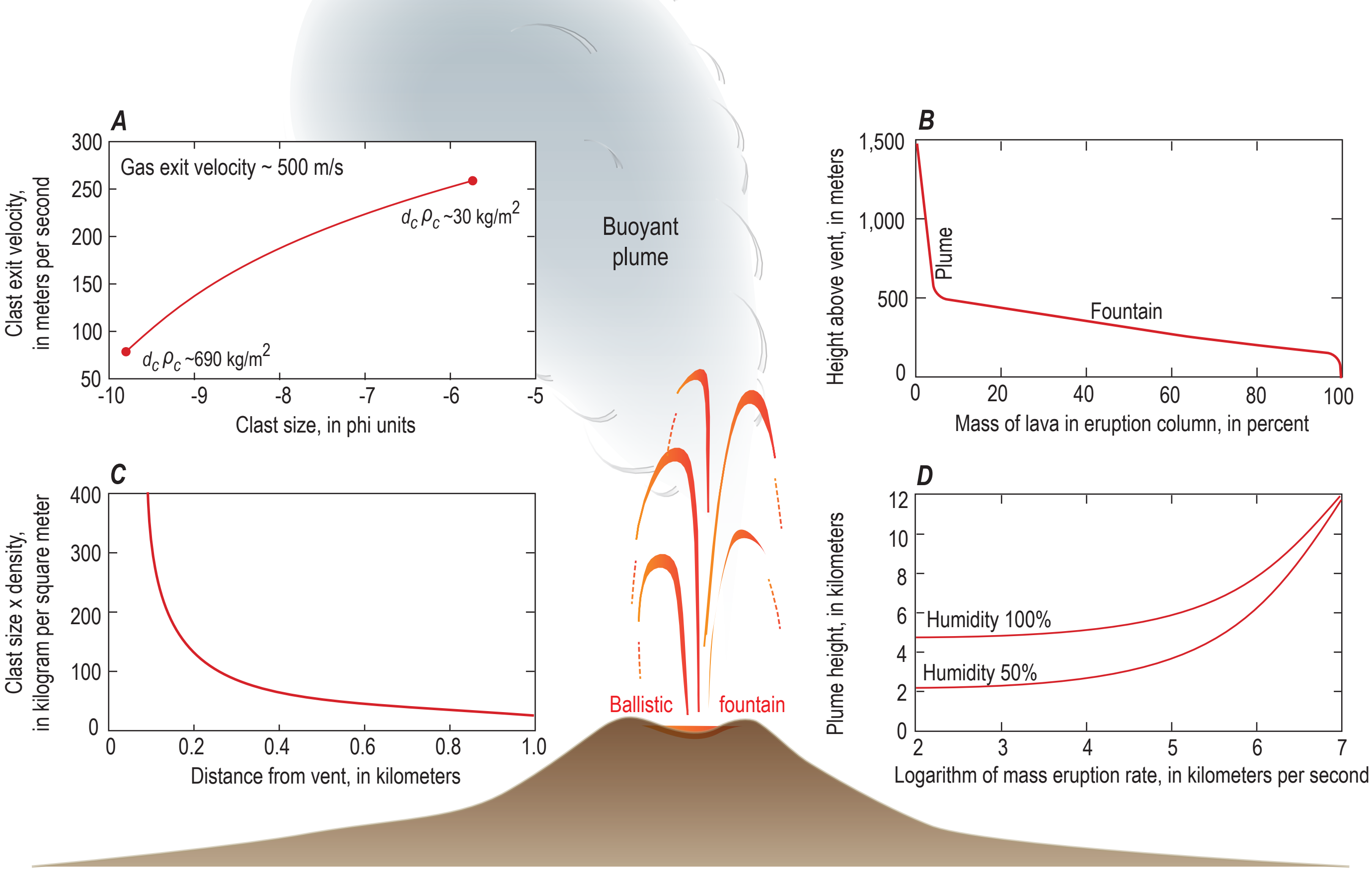

Figure 13. Diagram and graphs illustrating features of basaltic eruption columns. Ballistic region of the fountain contains a dispersion of centimeter- to meter-size molten clots rising tens to hundreds of meters at speeds less than that of gas. Above the fountain rises a buoyant plume of magmatic gas and aerosols, entrained air, and modest proportions of very fine ash. Unlike silicic plumes, which reach stratospheric heights, basaltic plumes are not expected to penetrate the tropopause. *A*, Clast exit velocity versus clast size (from Wilson, 1999), based on data from the 1959 Kīlauea Iki eruption. Modeled gas exit velocity of ~500 m/s exceeds that of clasts for all sizes shown. *B*, Mass percentage of clasts in eruption column versus height above vent, based on modeling of the Kīlauea Iki eruption by Parfitt and Wilson (1999). *C*, Density-modulated clast size (clast diameter, d_c, multiplied by clast density, ρ_c) versus lateral distance from the vent, based on modeling of the Kīlauea Iki eruption by Parfitt and Wilson (1999). *D*, Plume height versus logarithm of mass eruption rate at two different humidities (from Woods, 1993, and Sparks and others, 1997).

Basic plume theory gives the height, h_p, of a convecting plume as

$$h_p = 8.2Q^{1/4}, \quad (13)$$

where Q is the rate of thermal energy release as modulated by atmospheric conditions, the specific heats of magma and air, initial magma temperature, temperature decrease in the fountain due to cooling of pyroclasts, volumetric eruption rate, and the mass fractions of volatiles and fine lava fragments (see, for example, Sparks and Wilson, 1976; Wilson and others, 1978; Stothers and others, 1986; Woods, 1993; Sparks and others, 1997).

The flux of hot, juvenile ash adds significant buoyancy to silicic plumes but is a comparatively meager heat source for plumes above Hawaiian lava fountains, because ash is <5 percent of the total mass erupted (for example, Parfitt 1998). Likewise, the flux of hot magmatic volatiles released during fountaining episodes is "too small to have significant influence on column [plume] behavior" (Sparks and others, 1997). Basaltic plume models show that the amount of atmospheric water vapor incorporated into the fountain actually exceeds that of juvenile H_2O (Woods, 1993; Sparks and others, 1997). Entrainment of ambient water vapor adds significantly to buoyancy because, as the plume ascends into cooler atmospheric layers, condensation releases latent heat and decreases plume density (fig. 13*D*). The mass of entrained water vapor, m_a, is given by

$$m_a = m(C_m \Delta T)/(C_a(T_o - \Delta T)), \quad (14)$$

where C_m and C_a are the specific heats of magma and air, respectively, m is the eruptive mass flux, T_o is the initial eruption temperature, and ΔT is the temperature drop in the fountain. In tropical regions, where humidity is high, the added buoyancy can be substantial. Sparks and others (1997) calculated that the proportion of ambient water vapor entrained by basaltic lava fountains can be as much as 1–2 percent of the total mass in the fountain and an order of magnitude greater than the proportion of magmatic H_2O in the plume.

A "moist air" plume model (75–100 percent humidity) constructed by Woods (1993) and Sparks and others (1997) successfully reproduced the 7-km-high plume above the 1984 Mauna Loa vent by assuming ash fractions of 1–10 percent and using the known mass eruption rates (10^6 kg/s) and eruption temperatures (1,130 °C) of Lockwood and others (1984). A similar but "dry air" model (0 percent humidity) for the Mauna Loa plume constructed by Stothers and others (1986) underpredicted the Mauna Loa plume height by ~20 percent. Comparatively, entrained water vapor has the greatest effect on plume height at low mass eruption rates. At higher mass eruption rates, increasing proportions of cooler, less humid air from higher in the atmosphere are entrained (fig. 13*D*).

Dispersal Patterns

Airborne quenching of high-porosity pyroclasts is attributed to rapid, wholesale outgassing with simultaneous creation of an air-permeable network (for example, Wentworth and Macdonald, 1953; Mangan and Cashman, 1996; Namiki and Manga, 2008; Rust and Cashman, 2011). Clots too large for wholesale outgassing will continue to evolve upon deposition, their fate dictated by pyroclast temperature and local accumulation rates. Head and Wilson (1989) diagrammed post-deposition pyroclast evolution in the context of vent construction, delineating lava ponds, rootless lava flows, welded spatter, and loose scoria on the basis of pyroclast landing temperature and accumulation rate (fig. 14). Augmenting the diagrammatic approach of Head and Wilson with quantitative data on glass transition temperature for rapidly quenched basaltic melts (Potuzak and others, 2008), pyroclast quenching temperatures (Helz and Hearn, 1998), measured accumulation rates (Swanson and others, 1979; Heliker and others, 2003), and stratigraphically constrained componentry (Heliker and others, 2003) reveal the physical and thermal complexity of basaltic cones that form during episodic high fountaining from a central

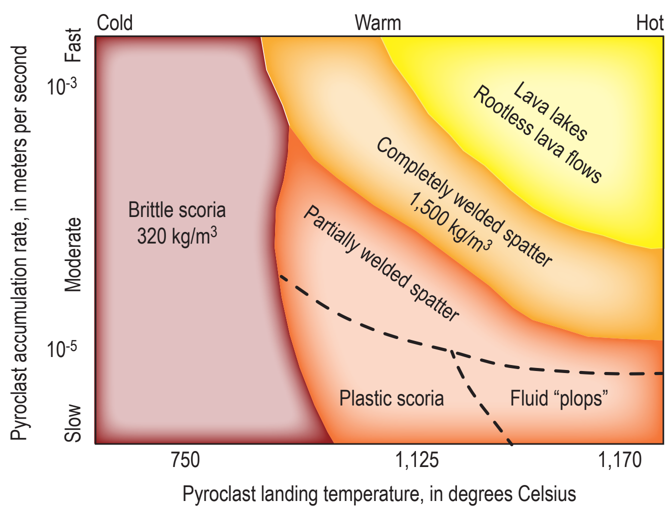

Figure 14. Plot of pyroclast accumulation rate versus landing temperature, illustrating the types of vent deposits produced during lava fountaining from a central vent. Values along the axes, which are not to scale, show the ranges in pyroclast landing temperature (olivine-glass geothermometry by Helz and Hearn, 1998, and basaltic glass calorimetry by Potuzak and others, 2008) and pyroclast accumulation rate (field measurements by Heliker and others, 2003). Vent deposits transition from loose accumulations of brittle scoria (bulk density ~320 kg/m^3) to mounds of completely welded spatter (bulk density ~1,500 kg/m^3) with increasing temperature and accumulation rate. At the highest values, falling pyroclasts coalesce upon landing, forming fluid lava lakes and (or) rootless lava flows. Plot modified from Head and Wilson (1989). Density data from Heliker and others (2003).

vent. Pyroclast landing temperatures may range from <750 °C (glass-transition temperature) to >1,170 °C (eruption temperature), and pyroclast-accumulation rates may range from $<10^{-5}$ to $>10^{-3}$ m/s, depending on mass eruption rate, fountain height, and windspeed. Steeper slopes characterize the downwind direction of the cone where deposits of unconsolidated scoria and welded spatter abound.

Heliker and others (2003) emphasize that the "cinder-and-spatter-cone[s]" created by high lava fountains are distinct from the cinder cones that result from eruptions of less fluid basalt (for example, during Strombolian- or Vulcanian-style eruptions). They described the 255-m-high Puʻu ʻŌʻō cone as a "striking landform . . . composed of cinder, agglutinated spatter, and lava flows." After 3 years and 44 high-fountain episodes, densely welded spatter and rootless lava flows composed more than three-quarters of its volume.

Though visually striking, the growing Puʻu ʻŌʻō cone represented only about 20 percent of the volume of lava emitted during fountaining episodes. Beyond the cone base, lava flows dominated, with distal ash fall contributing ≤2 percent of the eruptive volume. Typically, the sheetlike deposits of frothy pyroclasts and ash abruptly thin outward from the cone, generally diminishing to 10 percent of the maximum near-vent thickness over dispersal areas of <10 km².

A Look Toward the Future

> The predictability of the eruption process will depend on how well we can constrain the model parameters using the monitoring data.
>
> —*Keiiti Aki and Valérie Ferrazzini* (2000)

Pursuit of Jaggar's (1917) vision to "protect life and property on the basis of sound scientific achievement" in the 21st century calls for a new generation of eruption models with strength in hazard prediction. These models must be sufficiently sophisticated, multidisciplinary, and realistic to answer the vital questions: When and where will an eruption occur? What hazards are expected? How far afield will their impact be felt? How long will the hazard persist? Models must be adaptable to cover changing conditions and assess possible outcomes. Field-based studies must advance in tandem with model development, because real-world observations form the conceptual framework on which models are built.

Monitoring Instrumentation and Methodologies

Possibly most critically needed at present are investigations that more precisely constrain shallow conduit geometry and mixed-volatile degassing phenomena, because these parameters strongly influence the final ascent of magma and eruptive style. Research on Kīlauea since 2000 shows much promise on these fronts. In particular, small-aperture seismic and infrasound networks comprising instruments with a wide dynamic range are providing high-resolution mapping of the location and geometry of Kīlauea's shallow plumbing and degassing systems. Their value in conduit imaging is exemplified in recent studies integrating seismic and acoustic long-period, very-long-period, and tremor signals associated with the vigorous degassing that accompanied and followed the opening of the Halemaʻumaʻu vent in 2008 (Chouet and others, 2010; Dawson and others, 2010; Fee and others, 2010; Matoza and others, 2010; Chouet and Dawson, 2011; Patrick and others, 2011a). Seismic and acoustic signals, in combination with lidar (light detection and ranging) and FLIR (forward looking infrared radar) imaging, reveal conduit discontinuities at depths of ~1 km (a constriction) and ~200 m (flare opening to a cavity), which strongly influence eruptive patterns. The amplitude, period, and duration of signals are helping to determine flow patterns in the conduit and the distribution of gas. Particularly promising are recent efforts to correlate seismic and infrasound records with continuous infrared-spectroscopic monitoring of gas emissions (see Sutton and Elias, this volume, chap. 7). Since the start of renewed eruptive activity at Halemaʻumaʻu in 2008, gas compositions obtained by OP-FTIR show variations in CO_2/S ratio indicative of fluctuating depths of gas accumulation and varied mode of release.

Field Geology

Sophisticated and integrated monitoring networks are essential, but the role of traditional geologic investigations cannot be overlooked if predictive models are to have true utility. A prime example is afforded by recent studies of highly explosive eruptions through analysis of Kīlauea's tephra deposits. Although early workers, most notably Perret (1913d), Powers (1916), Stone (1926), Wentworth (1938), and Powers (1948), recognized Kīlauea's explosive past, modern follow-up studies have been limited to a few seminal investigations, including a summary of earlier observations by Decker and Christiansen (1984) and studies on tephra stratigraphy (McPhie and others, 1990; Dzurisin and others, 1995) and physical volcanology (Swanson and Christiansen, 1973; Dvorak, 1992; Mastin, 1997; Mastin and others, 2004).

In contrast to purely magmatic eruptions, research on phreatomagmatic (and phreatic) eruptions in Hawaiʻi is still in a discovery phase. Most or all of the most powerful explosive eruptions in Kilauea's past 2,500 years involved external water, including the eruption in 1790 that killed many people near the present location of HVO. Today's heightened interest comes from the realization that recurrence of such explosive activity could have severe consequences for the growing numbers of island residents and visitors—and that events in the past 2,000 years have sent ash into the jetstream, well within the flight altitudes of commercial aircraft (Swanson and others, 2011).

The hazards are all the more alarming in the context of recent findings showing that Kīlauea's explosive events have occurred more frequently and over longer periods of time than previously thought (Fiske and others, 2009; Swanson and others, 2012a, b). For example, new data from extensive ^{14}C dating and deposit analysis reveal that the widely known Keanakākoʻi Tephra, once believed to have been erupted in 1790, actually records a series of violent events spanning the period from ca. 1500 to the early 1800s (Swanson and others, 2012a, b). Moreover, these data suggest that Kīlauea's explosive activity is clustered over time. From 500 to 200 B.C.E., effusive eruptions dominated. This relatively benign era was followed by ~1,200 years of mostly explosive activity, a subsequent 500-year-long period of effusive activity, and then the ~300-year-long period of explosive eruptions responsible for the Keanakākoʻi Tephra, ending in the early 1800s. Effusive eruptions have dominated since, except for the small phreatic explosions of 1924. This notable cyclicity of different eruption styles is currently under intense study (Swanson and others, 2014).

Acknowledgments

We are grateful for many opportunities to share ideas and fieldwork with our colleagues at the Hawaiian Volcano Observatory, and are honored by their invitation to contribute to this collection of centennial papers. Many thanks to Tom Sisson and Matt Patrick for their constructive reviews of our chapter, and to Mike Poland, Jim Kauahikaua, Jane Takahashi, Manny Nathenson, George Havach, and Peter Stauffer for their help in editing. Our chapter also reaped the benefit of expert illustrations by Mae Marcaida and the gracious help of Bob Tilling, Tim Orr, Ben Gaddis, and Jane Takahashi in culling through HVO's photo archives. Layout and illustration refinements by Jeanne S. DiLeo.

References

Aki, K., and Ferrazzini, V., 2000, Seismic monitoring and modeling of an active volcano for prediction: Journal of Geophysical Research, v. 105, no. B7, p. 16617–16640, doi:10.1029/2000JB900033.

Aki, K., Fehler, M., and Das, S., 1977, Source mechanism of volcanic tremor; fluid-driven crack models and their application to the 1963 Kilauea eruption: Journal of Volcanology and Geothermal Research, v. 2, no. 3, p. 259–287, doi:10.1016/0377-0273(77)90003-8.

Allard, P., Burton, M., and Muré, F., 2005, Spectroscopic evidence for a lava fountain driven by previously accumulated magmatic gas: Nature, v. 433, no. 7024, p. 407–410, doi:10.1038/nature03246.

Babb, J.L., Kauahikaua, J.P., and Tilling, R.I., 2011, The story of the Hawaiian Volcano Observatory—A remarkable first 100 years of tracking eruptions and earthquakes: U.S. Geological Survey General Interest Product 135, 60 p. [Also available at http://pubs.usgs.gov/gip/135/.]

Becker, J.F., 1897, Some queries on rock differentiation: American Journal of Science, ser. 4, v. 3, no. 13, art. 3, p. 21–40, doi:10.2475/ajs.s4-3.13.21.

Bottinga, Y., and Javoy, M., 1990, Mid-ocean ridge basalt degassing; bubble nucleation: Journal of Geophysical Research, v. 95, no. B4, p. 5125–5131, doi:10.1029/JB095iB04p05125.

Bottinga, Y., and Javoy, M., 1991, The degassing of Hawaiian tholeiite: Bulletin of Volcanology, v. 53, no. 2, p. 73–85, doi:10.1007/BF00265413.

Bottinga, Y., and Weill, D.F., 1972, The viscosity of magmatic silicate liquids; a model for calculation: American Journal of Science, v. 272, no. 5, p. 438–475, doi:10.2475/ajs.272.5.438.

Bruce, P.M., and Huppert, H.E., 1989, Thermal control of basaltic fissure eruptions: Nature, v. 342, no. 6250, p. 665–667, doi:10.1038/342665a0.

Bruce, P.M., and Huppert, H.E., 1990, Solidification and melting along dykes by the laminar flow of basaltic magma, chap. 6 *of* Ryan, M.P., ed., Magma transport and storage: Chichester, U.K., John Wiley & Sons, p. 87–102. [Also available at http://www.itg.cam.ac.uk/people/heh/Paper96.pdf.]

Brun, A., 1911, Volcans des Îles Sandwich; Kilauea (Halemaumau), chap. 4 *of* Recherches sur l'exhalaison volcanique: Geneva, Librairie Kundig, p. 232–253.

Cashman, K.V., and Mangan, M.T., 1994, Physical aspects of magmatic degassing; II. Constraints on vesiculation processes from textural studies of eruptive products, chap. 11b *of* Carroll, M.R., and Holloway, J.R., eds., Volatiles in magmas: Reviews in Mineralogy, v. 30, p. 447–478.

Cashman, K.V., and Marsh, B.D., 1988, Crystal size distribution (CSD) in rocks and the kinetics of dynamics of crystallization: Contributions to Mineralogy and Petrology, v. 99, no. 3, p. 292–305, doi:10.1007/BF00375363.

Cashman, K.V., Sturtevant, B., Papale, P., and Navon, O., 2000, Magmatic fragmentation, *in* Sigurdsson, H., Houghton, B.F., McNutt, S.R., Rymer, H., and Styx, J., eds., Encyclopedia of volcanoes: San Diego, Calif., Academic Press, p. 421–430.

Chouet, B., and Dawson, P., 2011, Shallow conduit system at Kilauea Volcano, Hawaii, revealed by seismic signals associated with degassing bursts: Journal of Geophysical Research, v. 116, B12317, 22 p., doi:10.1029/2011JB008677.

Chouet, B.A., Dawson, P.B., James, M.R., and Lane, S.J., 2010, Seismic source mechanism of degassing bursts at Kilauea Volcano, Hawaii; results from waveform inversion in the 10–50 s band: Journal of Geophysical Research, v. 115, B09311, 24 p., doi:10.1029/2009JB006661.

Costantini, L., Bonadonna, C., Houghton, B.F., and Wehrmann, H., 2009, New physical characterization of the Fontana Lapilli basaltic Plinian eruption, Nicaragua: Bulletin of Volcanology, v. 71, no. 3, p. 337–355, doi:10.1007/s00445-008-0227-9.

Costantini, L., Houghton, B.F., and Bonadonna, C., 2010, Constraints on eruption dynamics of basaltic explosive activity derived from chemical and microtextural study; the example of the Fontana Lapilli Plinian eruption, Nicaragua: Journal of Volcanology and Geothermal Research, v. 189, nos. 3–4, p. 207–224, doi:10.1016/j.jvolgeores.2009.11.008.

Crisp, J., Cashman, K.V., Bonini, J.A., Hougen, S.B., and Pieri, D.C., 1994, Crystallization history of the 1984 Mauna Loa lava flow: Journal of Geophysical Research, v. 99, no. B4, p. 7177–7198, doi:10.1029/93JB02973.

Daly, R.A., 1911, The nature of volcanic action: Proceedings of the American Academy of Arts and Sciences, v. 47, p. 47–122, pls.,10 p., accessed May 31, 2013, at http://www.jstor.org/stable/20022712.

Dana, J.D., 1890, Characteristics of volcanoes, with contributions of facts and principles from the Hawaiian Islands; including a historical review of Hawaiian volcanic action for the past sixty-seven years, a discussion of the relations of volcanic islands to deep-sea topography, and a chapter on volcanic-island denudation: New York, Dodd, Mead, and Co., 399 p.

Daniels, K.A., Kavanagh, J.L., Menard, T., and Sparks, R.S.J., 2012, The shape of dikes; evidence for the influence of cooling and inelastic deformation: Geological Society of America Bulletin, v. 124, nos. 7–8, p. 1102–1112, doi:10.1130/B30537.1.

Dawson, P.B., Benitez, M.C., Chouet, B.A., Wilson, D., and Okubo, P.G., 2010, Monitoring very-long-period seismicity at Kilauea Volcano, Hawaii: Geophysical Research Letters, v. 37, no. 18, L18306, 5 p., doi:10.1029/2010GL044418.

Day, A.L., and Shepherd, E.S., 1913, Water and volcanic activity: Geological Society of America Bulletin, v. 24, December 16, p. 573–606.

de Vries, A.J., 1972, Morphology, coalescence, and size distribution of foam bubbles, chap. 2 *of* Lemlich, R., ed., Adsorptive bubble separation techniques: New York, Academic Press, p. 7–31.

Decker, R.W., and Christiansen, R.L., 1984, Explosive eruptions of Kilauea Volcano, Hawaii, *in* National Research Council, ed., Explosive volcanism; inception, evolution and hazards: Washington, D.C., National Academy Press, p. 122–132. [Also available at http://hdl.handle.net/10524/23399].

Delaney, P.T., and Pollard, D.D., 1981, Deformation of host rocks and flow of magma during growth of minette dikes and breccia-bearing intrusions near Ship Rock, New Mexico: U.S. Geological Survey Professional Paper 1202, 61 p., accessed March 6, 2013, at http://pubs.usgs.gov/pp/1202/.

Delaney, P.T., and Pollard, D.D., 1982, Solidification of basaltic magma during flow in a dike: American Journal of Science, v. 282, no. 6, p. 856–885, doi:10.2475/ajs.282.6.856.

Dvorak, J.J., 1992, Mechanism of explosive eruptions of Kilauea Volcano, Hawaii: Bulletin of Volcanology, v. 54, no. 8, p. 638–645, doi:10.1007/BF00430777.

Dvorak, J.J., Okamura, A.T., English, T.T., Koyanagi, R.Y., Nakata, J.S., Sako, M.K., Tanigawa, W.T., and Yamashita, K.M., 1986, Mechanical response of the south flank of Kilauea volcano, Hawaii, to intrusive events along the rift systems: Tectonophysics, v. 124, nos. 3–4, p. 193–209, doi:10.1016/0040-1951(86)90200-3.

Dzurisin, D., Lockwood, J.P., Casadevall, T.J., and Rubin, M., 1995, The Uwekahuna Ash Member of the Puna Basalt; product of violent phreatomagmatic eruptions at Kilauea volcano between 2,800 and 2,100 ^{14}C years ago: Journal of Volcanology and Geothermal Research, v. 66, nos. 1–4, p. 163–184, doi:10.1016/0377-0273(94)00062-L.

Eaton, J.P., 1962, Crustal structure and volcanism in Hawaii, *in* Macdonald, G.A., and Kuno, H., eds., Crust of the Pacific Basin: American Geophysical Union Geophysical Monograph 6, p. 13–29, doi:10.1029/GM006p0013.

Eaton, J.P., and Murata, K.J., 1960, How volcanoes grow: Science, v. 132, no. 3432, p. 925–938, doi:10.1126/science.132.3432.925.

Edmonds, M., and Gerlach, T.M., 2007, Vapor segregation and loss in basaltic melts: Geology, v. 35, no. 8, p. 751–754, doi:10.1130/G23464A.1.

Ellis, A.J., 1957, Chemical equilibrium in magmatic gases: American Journal of Science, v. 255, no. 6, p. 416–431, doi:10.2475/ajs.255.6.416.

Fee, D., Garcés, M., Patrick, M., Chouet, B., Dawson, P., and Swanson, D., 2010, Infrasonic harmonic tremor and degassing bursts from Halema’uma’u Crater, Kilauea Volcano, Hawaii: Journal of Geophysical Research, v. 115, no. B11316, 15 p., doi:10.1029/2010JB007642.

Ferrazzini, V., Aki, K., and Chouet, B., 1991, Characteristics of seismic waves composing Hawaiian volcanic tremor and gas-piston events observed by a near-source array: Journal of Geophysical Research, v. 96, no. B4, p. 6199–6209, doi:10.1029/90JB02781.

Finlayson, J.B., Barnes, I.L., and Naughton, J.J., 1968, Developments in volcanic gas research in Hawaii, *in* Knopoff, L., Drake, C.L., and Hart, P.J., eds., The crust and upper mantle of the Pacific area: American Geophysical Union Geophysical Monograph 12, p. 428–438.

Fiske, R.S., and Kinoshita, W.T., 1969, Inflation of Kilauea volcano prior to its 1967–1968 eruption: Science, v. 165, no. 3891, p. 341–349, doi:10.1126/science.165.3891.341.

Fiske, R.S., Rose, T.R., Swanson, D.A., Champion, D.E., and McGeehin, J.P., 2009, Kulanaokuaiki Tephra (ca. A.D. 400–1000); newly recognized evidence for highly explosive eruptions at Kīlauea Volcano, Hawai‘i: Geological Society of America Bulletin, v. 121, nos. 5–6, p. 712–728, doi:10.1130/B26327.1.

Frenkel, J., 1955, Kinetic theory of liquids: New York, Dover Publications, 485 p.

Gerlach, T.M., 1980, Evaluation of volcanic gas analyses from Kilauea volcano, *in* McBirney, A.R., ed., Gordon A. Macdonald memorial volume: Journal of Volcanology and Geothermal Research, v. 7, nos. 3–4 (special issue), p. 295–317, doi:10.1016/0377-0273(80)90034-7.

Gerlach, T.M., 1986, Exsolution of H_2O, CO_2, and S during eruptive episodes at Kilauea Volcano, Hawaii: Journal of Geophysical Research, v. 91, no. B12, p. 12177–12185, doi:10.1029/JB091iB12p12177.

Gerlach, T.M., and Graeber, E.J., 1985, Volatile budget of Kilauea volcano: Nature, v. 313, no. 6000, p. 273–277, doi:10.1038/313273a0.

Gerlach, T.M., and Nordlie, B.E., 1975a, The C-O-H-S gaseous system; part I, Composition limits and trends in basaltic cases: American Journal of Science, v. 275, no. 4, p. 353–376, doi:10.2475/ajs.275.4.353.

Gerlach, T.M., and Nordlie, B.E., 1975b, The C-O-H-S gaseous system; part II, Temperature, atomic composition, and molecular equilibria in volcanic gases: American Journal of Science, v. 275, no. 4, p. 377–394, doi:10.2475/ajs.275.4.377.

Gerlach, T.M., and Nordlie, B.E., 1975c, The C-O-H-S gaseous system; part III, Magmatic gases compatible with oxides and sulfides in basaltic magmas: American Journal of Science, v. 275, no. 4, p. 395–410, doi:10.2475/ajs.275.4.395.

Gerlach, T.M., McGee, K.A., Elias, T., Sutton, A.J., and Doukas, M.P., 2002, Carbon dioxide emission rate of Kīlauea Volcano; implications for primary magma and the summit reservoir: Journal of Geophysical Research, v. 107, no. B9, 2189, 15 p., doi:10.1029/2001JB000407.

Giggenbach, W.F., 1975, A simple method for the collection and analysis of volcanic gas samples: Bulletin Volcanologique, v. 39, no. 1, p. 132–145, doi:10.1007/BF02596953.

Green, W.L., 1887, Vestiges of the molten globe; part II. The Earth’s surface features and volcanic phenomena: Honolulu, Hawaiian Gazette, 337 p.

Greenland, L.P., 1988, Gases from the 1983–1984 east-rift eruption, chap. 4 *of* Wolfe, E.W., ed., The Puu Oo eruption of Kilauea Volcano, Hawaii; episodes 1 through 20, January 3, 1983, through June 8, 1984: U.S. Geological Survey Professional Paper 1463, p. 145–153. [Also available at http://pubs.usgs.gov/pp/1463/report.pdf.]

Greenland, L.P., Rose, W.I., and Stokes, J.B., 1985, An estimate of gas emissions and magmatic gas content from Kilauea Volcano: Geochimica et Cosmochimica, v. 49, no. 1, p. 125–129, doi:10.1016/0016-7037(85)90196-6.

Greenland, L.P., Okamura, A.T., and Stokes, J.B., 1988, Constraints on the mechanics of the eruption, chap. 5 *of* Wolfe, E.W., ed., The Puu Oo eruption of Kilauea Volcano, Hawaii; episodes 1 through 20, January 3, 1983, through June 8, 1984: U.S. Geological Survey Professional Paper 1463, p. 155–164. [Also available at http://pubs.usgs.gov/pp/1463/report.pdf.]

Hardee, H.C., 1987, Heat and mass transport in the east rift zone magma conduit of Kilauea Volcano, chap. 54 *of* Decker, R.W., Wright, T.L., and Stauffer, P.H., eds., Volcanism in Hawaii: U.S. Geological Survey Professional Paper 1350, v. 2, p. 1471–1486. [Also available at http://pubs.usgs.gov/pp/1987/1350/.]

Harris, A.J.L., and Allen, J.S., 2008, One, two, and three-phase viscosity measurements for basaltic lava flows: Journal of Geophysical Research, v. 113, B09212, 15 p., doi:10.1029/2007JB005035.

Hass, P.A., and Johnson, H.F., 1967, A model and experimental results for drainage of solution between foam bubbles: Industrial & Engineering Chemical Fundamentals, v. 6, no. 2, p. 225–233, doi:10.1021/i160022a010.

Head, J.W., III, and Wilson, L., 1987, Lava fountain heights at Pu‘u ‘O‘o, Kilauea, Hawaii; indicators of amount and variations of exsolved magma volatiles: Journal of Geophysical Research, v. 92, no. B13, p. 13715–13719, doi:10.1029/JB092iB13p13715.

Head, J.W., III, and Wilson, L., 1989, Basaltic pyroclastic eruptions; influence of gas-release patterns and volume fluxes on fountain structure, and the formation of cinder cones, spatter cones, rootless flows, lava ponds and lava flows: Journal of Volcanology and Geothermal Research, v. 37, nos. 3–4, p. 261–271, doi:10.1016/0377-0273(89)90083-8.

Heald, E.F., 1963, The chemistry of volcanic gases; 2. Use of equilibrium calculations in the interpretation of volcanic gas samples: Journal of Geophysical Research, v. 68, no. 2, p. 545–557, doi:10.1029/JZ068i002p00545.

Heald, E.F., and Naughton, J.J., 1962, Calculation of chemical equilibria in volcanic systems by means of computers: Nature, v. 193, no. 4816, p. 642–644, doi:10.1038/193642a0.

Heliker, C.C., and Mattox, T.N., 2003, The first two decades of the Pu‘u ‘Ō‘ō-Kūpaianaha eruption; chronology and selected bibliography, *in* Heliker, C.C., Swanson, D.A., and Takahashi, T.J., eds., The Pu‘u ‘Ō‘ō-Kūpaianaha eruption of Kīlauea Volcano, Hawai‘i; the first 20 years: U.S. Geological Survey Professional Paper 1676, p. 1–27. [Also available at http://pubs.usgs.gov/pp/pp1676/.]

Heliker, C.C., and Wright, T.L., 1991, The Pu’u ‘O’o-Kupaianaha eruption of Kilauea: Eos (American Geophysical Union Transactions), v. 72, no. 47, p. 521, 526, 530, doi:10.1029/90EO00372.

Heliker, C.C., Kauahikaua, J.P., Sherrod, D.R., Lisowski, M., and Cervelli, P.F., 2003, The rise and fall of Pu‘u ‘Ō‘ō cone, 1983–2002, *in* Heliker, C.C., Swanson, D.A., and Takahashi, T.J., eds., The Pu‘u ‘Ō‘ō-Kūpaianaha eruption of Kīlauea Volcano, Hawai‘i; the first 20 years: U.S. Geological Survey Professional Paper 1676, p. 29–52. [Also available at http://pubs.usgs.gov/pp/pp1676/.]

Helz, R.T., 1987, Diverse olivine types in lava of the 1959 eruption of Kilauea Volcano and their bearing on eruption dynamics, chap. 25 *of* Decker, R.W., Wright, T.L., and Stauffer, P.H., eds., Volcanism in Hawaii: U.S. Geological Survey Professional Paper 1350, v. 1, p. 691–722. [Also available at http://pubs.usgs.gov/pp/1987/1350/.]

Helz, R.T., and Hearn, B.C., Jr., 1998, Compositions of glasses from the Pu’u O’o-Kupaianaha eruption of Kilauea volcano, Hawaii, January 1983 through December 1994: U.S. Geological Survey Open-File Report 98–511, 77 p. [Also available at http://pubs.usgs.gov/of/1998/0511/report.pdf.]

Helz, R.T., Clague, D.A., Mastin, L.G., and Rose, T.R., in press, Evidence for large compositional ranges in coeval melts erupted from Kīlauea’s summit reservoir: American Geophysical Union Chapman Monograph.

Helz, R.T., Clague, D.A., Sisson, T.W., and Thornber, C.R., 2014, Petrologic insights into basaltic volcanism, chap. 6 *of* Poland, M.P., Takahashi, T.J., and Landowski, C.M., eds., Characteristics of Hawaiian volcanoes: U.S. Geological Survey Professional Paper 1801 (this volume).

Herd, R.A., and Pinkerton, H., 1997, Bubble coalescence in basaltic lava; its impact on the evolution of bubble populations: Journal of Volcanology and Geothermal Research, v. 75, no. 1–2, p. 137–157, doi:10.1016/S0377-0273(96)00039-X.

Hill, D.P., 1977, A model for earthquake swarms: Journal of Geophysical Research, v. 82, no. 8, p. 1347–1531, doi:10.1029/JB082i008p01347.

Hitchcock, C.H., 1911, Hawaii and its volcanoes (2d ed.): Honolulu, Hawaiian Gazette, 314 p., supplement, p. 1–8, 1 pl. [supplement interleaved between p. 306 and 307].

Hoffmann, J.P., Ulrich, G.E., and Garcia, M.O., 1990, Horizontal ground deformation patterns and magma storage during the Puu Oo eruption of Kilauea volcano, Hawaii; episodes 22–42: Bulletin of Volcanology, v. 52, no. 7, p. 522–531, doi:10.1007/BF00301533.

Houghton, B.F., and Gonnerman, H.M., 2008, Basaltic explosive volcanism; constraints from deposits and models: Chemie der Erde Geochemistry, v. 68, no. 2, p. 117–140, doi:10.1016/j.chemer.2008.04.002.

Houghton, B.F., and Wilson, C.J.N., 1989, A vesicularity index for pyroclastic deposits: Bulletin of Volcanology, v. 51, no. 6, p. 451–462, doi:10.1007/BF01078811.

Houghton, B.F., Swanson, D.A., Carey, R.J., Rausch, J., and Sutton, A.J., 2011, Pigeonholing pyroclasts; insights from the 19 March 2008 explosive eruption of Kīlauea volcano: Geology, v. 39, no. 3, p. 263–266, doi:10.1130/G31509.1.

Ivanov, I.B., and Dimitrov, D.S., 1988, Thin film drainage, chap. 7 *of* Ivanov, I.B., ed., Thin liquid films; fundamentals and applications: New York, Marcel Dekker, p. 379–495.

Jaggar, T.A., Jr., 1917, Volcanologic investigations at Kilauea: American Journal of Science, ser. 4, v. 44, no. 261, art. 16, p. 161–220, doi:10.2475/ajs.s4-44.261.161.

Jaggar, T.A., Jr., 1940, Magmatic gases: American Journal of Science, v. 238, no. 5, p. 313–353, doi:10.2475/ajs.238.5.313.

Jaggar, T.A., Jr., 1945, Volcanoes declare war; logistics and strategy of Pacific volcano science: Honolulu, Paradise of the Pacific, 166 p.

James, M.R., Lane, S.J., and Corder, S.B., 2008, Modeling the rapid near-surface expansion of gas slugs in low-viscosity magmas, *in* Lane, S.J., and Gilbert, J.S., eds., Fluid motions in volcanic conduits; a source of seismic and acoustic signals: Geological Society of London Special Publication 307, p. 147–167, doi:10.1144/SP307.9.

Jaupart, C., 2000, Magma ascent at shallow levels, *in* Sigurdsson, H., Houghton, B.F., McNutt, S.R., Rymer, H., and Styx, J., eds., Encyclopedia of volcanoes: San Diego, Calif., Academic Press, p. 237–245.

Jaupart, C., and Vergniolle, S., 1988, Laboratory models of Hawaiian and Strombolian eruptions: Nature, v. 331, no. 6151, p. 58–60, doi:10.1038/331058a0.

Johnson, J.B., Harris, A.J.L., and Hoblitt, R.P., 2005, Thermal observations of gas pistoning at Kilauea Volcano: Journal of Geophysical Research, v. 110, no. B11, 12 p., B11201, doi:10.1029/2005JB003944.

Kauahikaua, J.P., Mangan, M.T., Heliker, C.C., and Mattox, T., 1996, A quantitative look at the demise of a basaltic vent; the death of Kupaianaha, Kilauea Volcano, Hawai‘i: Bulletin of Volcanology, v. 57, no. 8, p. 641–648, doi:10.1007/s004450050117.

Khitarov, N.I., Lebedev, Y.B., Dorfman, A.M., and Bagdassarov, N.S., 1979, Effects of temperature, pressure and volatiles on the surface tension of molten basalt: Geochemistry International, v. 16, no. 5, p. 78–86.

Kinsley, J., 1931, The viscosity of lava: Volcano Letter, no. 357, October 29, p. 1–2. (Reprinted in Fiske, R.S., Simkin, T., and Nielsen, E., eds., 1987, The Volcano Letter: Washington, D.C., Smithsonian Institution Press, n.p.)

Klein, F.W., Koyanagi, R.Y., Nakata, J.S., and Tanigawa, W.R., 1987, The seismicity of Kilauea’s magma system, chap. 43 *of* Decker, R.W., Wright, T.L., and Stauffer, P.H., eds., Volcanism in Hawaii: U.S. Geological Survey Professional Paper 1350, v. 2, p. 1019–1185. [Also available at http://pubs.usgs.gov/pp/1987/1350/.]

Lautze, N.C., Sisson, T.W., Mangan, M.T., and Grove, T.L., 2011, Segregating gas from melt; an experimental study of Ostwald ripening of vapor bubbles in magmas: Contributions to Mineralogy and Petrology, v. 161, no. 2, p. 331–347, doi:10.1007/s00410-010-0535-x. (Erratum and correction published in this issue, p. 349, doi:10.1007/s00410-010-0563-6.)

Lister, J.R., and Kerr, R.C., 1991, Fluid-mechanical models of crack propagation and their application to magma transport in dykes: Journal of Geophysical Research, v. 96, no. B6, p. 10049–10077, doi:10.1029/91JB00600.

Llewellin, E.W., and Manga, M., 2005, Bubble suspension rheology and implications for conduit flow, *in* Sahagian, D., ed., Volcanic eruption mechanisms; insights from intercomparison of models of conduit processes: Journal of Volcanology and Geothermal Research, v. 143, nos. 1–3, p. 205–217, doi:10.1016/j.jvolgeores.2004.09.018.

Lockwood, J., USGS Hawaiian Volcano Observatory Staff, Rhodes, J.M., Garcia, M., Casadavall, T., Krueger, A., and Matson, M., 1984, Mauna Loa Volcano: SEAN Bulletin, v. 9, no. 3, p. 2–9.

Macdonald, G.A., 1954, Activity of Hawaiian volcanoes during the years 1940–1950: Bulletin Volcanologique, v. 15, no. 1, p. 119–179, doi:10.1007/BF02596001.

Macdonald, G.A., 1955, Hawaiian volcanoes during 1952: U.S. Geological Survey Bulletin 1021–B, p. 15–108, 14 pls. [Also available at http://pubs.usgs.gov/bul/1021b/report.pdf.]

Macdonald, G.A., 1963, Physical properties of erupting Hawaiian magmas: Geological Society of America Bulletin, v. 74, no. 8, p. 1071–1078, doi:10.1130/0016-7606(1963)74[1071:PPOEHM]2.0.CO;2.

Mader, H.M., Brodsky, E.E., Howard, D., and Sturtevant, B., 1997, Laboratory simulations of sustained volcanic eruptions: Nature, v. 388, no. 6641, p. 462–464, accessed June 3, 2013, at http://www.nature.com/nature/journal/v388/n6641/pdf/388462a0.pdf.

Manga, M., and Loewenberg, M., 2001, Viscosity of magma containing highly deformable bubbles: Journal of Volcanology and Geothermal Research, v. 105, no. 1, p. 19–24, doi:10.1016/S0377-0273(00)00239-0.

Manga, M.T., and Stone, H.A., 1994, Interactions between bubbles in magmas and lavas; effects of bubble deformation: Journal of Volcanology and Geothermal Research, v. 63, nos. 3–4, p. 267–279, doi:10.1016/0377-0273(94)90079-5.

Manga, M., Castro, J., Cashman, K.V., and Lowenberg, M., 1998, Rheology of bubble-bearing magmas: Journal of Volcanology and Geothermal Research, v. 87, p. 15–28, doi:10.1016/S0377-0273(98)00091-2.

Mangan, M.T., and Cashman, K.V., 1996, The structure of basaltic scoria and reticulite and inferences for vesiculation, foam formation, and fragmentation in lava fountains: Journal of Volcanology and Geothermal Research, v. 73, no. 1–2, p. 1–18, doi:10.1016/0377-0273(96)00018-2.

Mangan, M.T., Cashman, K.V., and Newman, S., 1993, Vesiculation of basaltic magma during eruption: Geology, v. 21, no. 2, p. 157–160, doi:10.1130/0091-7613(1993)021<0157:VOBMDE>2.3.CO;2.

Mangan, M.T., Sisson, T., and Hankins, B., 2006, Deep carbon dioxide-rich degassing of Pavlof Volcano, Aleutian arc [abs.]: American Geophysical Union, fall meeting 2006 Abstracts, no. V34A–01, accessed April 28, 2014, at http://abstractsearch.agu.org/meetings/2006/FM/sections/V/sessions/V34A/abstracts/V34A-01.html.

Mastin, L.G., 1997, Evidence for water influx from a caldera lake during the explosive hydromagmatic eruption of 1790, Kilauea volcano, Hawaii: Journal of Geophysical Research, v. 102, no. B9, p. 20093–20109, doi:10.1029/97JB01426.

Mastin, L.G., and Ghiorso, M.S., 2000, A numerical program for steady-state flow of magma-gas mixtures through vertical eruptive conduits: U.S. Geological Survey Open-File Report 00–209, 53 p. [Also available at http://vulcan.wr.usgs.gov/Projects/Mastin/Publications/OFR00-209/OFR00-209.pdf.]

Mastin, L.G., Christiansen, R.L., Thornber, C., Lowenstern, J., and Beeson, M., 2004, What makes hydromagmatic eruptions violent? Some insights from the Keanakāko'i Ash, Kīlauea volcano, Hawai'i: Journal of Volcanology and Geothermal Research, v. 137, nos. 1–3, p. 115–31, doi:10.1016/j.jvolgeores.2004.05.015.

Matoza, R.S., Fee, D., and Garcés, M.A., 2010, Infrasonic tremor wavefield of the Pu`u `Ō`ō crater complex and lava tube system, Hawaii, in April 2007: Journal of Geophysical Research, v. 115, B12312, 16 p., doi:10.1029/2009JB007192.

Matsuo, S., 1962, Establishment of chemical equilibrium in the volcanic gas obtained from the lava lake of Kilauea, Hawaii: Bulletin Volcanologique, v. 24, no. 1, p. 59–71, doi:10.1007/BF02599329.

McBirney, A.R., 1963, Factors governing the nature of submarine volcanism: Bulletin Volcanologique, v. 26, no. 1, p. 455–469, doi:10.1007/BF02597304.

McBirney, A.R., and Murase, T., 1970, Factors governing the formation of pyroclastic rocks: Bulletin Volcanologique, v. 34, no. 2, p. 372–384, doi:10.1007/BF02596762.

McPhie, J., Walker, G.P.L., and Christiansen, R.L., 1990, Phreatomagmatic and phreatic fall and surge deposits from explosions at Kilauea volcano, Hawaii, 1790 A.D.; Keanakakoi Ash Member: Bulletin of Volcanology, v. 52, no. 5, p. 334–354, doi:10.1007/BF00302047.

Moitra, P., Gonnermann, H.M., Houghton, B.F., and Giachetti, T., 2013, Relating vesicle shapes in pyroclast to eruption styles: Bulletin of Volcanology, v. 75, no. 2, p. 1–14, doi:10.1007/s00445-013-0691-8.

Murase, T., and McBirney, A.R., 1973, Properties of some common igneous rocks and their melts at high temperatures: Geological Society of America Bulletin, v. 84, no. 11, p. 3563–3592, doi:10.1130/0016-7606(1973)84<3563:POSCIR>2.0.CO;2.

Murata, K.J., 1966, An acid fumarolic gas from Kilauea Iki, Hawaii, *in* The 1959–60 eruption of Kilauea volcano, Hawaii: U.S. Geological Survey Professional Paper 537–C, p. C1–C6. [Also available at http://pubs.usgs.gov/pp/0537c/report.pdf.]

Murata, K.J., and Richter, D.H., 1966, Chemistry of the lavas of the 1959–60 eruption of Kilauea Volcano, Hawaii, *in* The 1959–60 eruption of Kilauea volcano, Hawaii: U.S. Geological Survey Professional Paper 537–A, p. A1–A26. [Also availab le at http://pubs.usgs.gov/pp/0537a/report.pdf].

Namiki, A., and Mangan, M., 2008, Transition between fragmentation and permeable outgassing of low viscosity magma: Journal of Volcanology and Geothermal Research, v. 169, nos. 1–2, p. 48–60, doi:10.1016/j.jvolgeores.2007.07.020.

Naughton, J.J., Heald, E.F., and Barnes, I.L., Jr., 1963, The chemistry of volcanic gases; 1. Collection and analysis of equilibrium mixtures by gas chromatograpy: Journal of Geophysical Research, v. 68, no. 2, p. 539–544, doi:10.1029/JZ068i002p00539.

Naughton, J.J., Derby, J., and Glover, R., 1969, Infrared measurements on volcanic gas and fume; Kilauea eruption, 1968: Journal of Geophysical Research, v. 74, no. 12, p. 3273–3277, doi:10.1029/JB074i012p03273.

Orr, T.R., and Rea, J.C., 2012, Time-lapse camera observations of gas piston activity at Pu'u 'O'o, Kīlauea volcano, Hawai'i: Bulletin of Volcanology, v. 74, no. 10, p. 2353–2362, doi:10.1007/s00445-012-0667-0.

Pal, R., 2003, Rheological behavior of bubble bearing magmas: Earth and Planetary Science Letters, v. 207, nos. 1–4, p. 165–179, doi:10.1016/S0012-821X(02)01104-4.

Palmer, H.S., 1927, A study of the viscosity of lava: Monthly Bulletin of the Hawaiian Volcano Observatory, v. 15, no. 1, p. 1–4. (Reprinted in Bevens, D., Takahashi, T.J., and Wright, T.L., eds., 1988, The early serial publications of the Hawaiian Volcano Observatory: Hawaii National Park, Hawaii, Hawai'i Natural History Association, v. 3, p. 919–922.)

Papale, P., Neri, A., Macedonio, G., 1998, The role of magma composition and water content in explosive eruptions: I. Conduit ascent dynamics: Journal of Volcanology and Geothermal Research, v. 87, nos. 1–4, p. 75–93, doi:10.1016/S0377-0273(98)00101-2.

Parcheta, C.E., Houghton, B.F., and Swanson, D.A., 2013, Contrasting patterns of vesiculation in low, intermediate, and high Hawaiian fountains; a case study of the 1969 Mauna Ulu eruption: Journal of Volcanology and Geothermal Research, v. 255, April 1, p. 79–89, doi:10.1016/j.jvolgeores.2013.01.016.

Parfitt, E.A., 1998, A study of clast size distribution, ash deposition and fragmentation in a Hawaiian-style volcanic eruption: Journal of Volcanology and Geothermal Research, v. 84, nos. 3–4, p. 197–208, doi:10.1016/S0377-0273(98)00042-0.

Parfitt, E.A., 2004, A discussion of the mechanisms of explosive basaltic eruptions: Journal of Volcanology and Geothermal Research, v. 134, nos. 1–2, p. 77–107, doi:10.1016/j.jvolgeores.2004.01.002.

Parfitt, E.A., and Wilson, L., 1994, The 1983–86 Pu´u ´O´o eruption of Kilauea volcano, Hawaii; a study of dike geometry and eruption mechanisms for a long-lived eruption: Journal of Volcanology and Geothermal Research, v. 59, no. 3, p. 179–205, doi:10.1016/0377-0273(94)90090-6.

Parfitt, E.A., and Wilson, L., 1995, Explosive volcanic eruptions—IX. The transition between Hawaiian-style and lava fountaining and Strombolian explosive activity: Geophysical Journal International, v. 121, no. 1, p. 226–232, doi:10.1111/j.1365-246X.1995.tb03523.x.

Parfitt, E.A., and Wilson, L., 1999, A Plinian treatment of fallout from Hawaiian lava fountains: Journal of Volcanology and Geothermal Research, v. 88, nos. 1–2, p. 67–75, doi:10.1016/S0377-0273(98)00103-6.

Parfitt, E.A., and Wilson, L., 2008, Fundamentals of physical volcanology: Oxford, U.K., Blackwell Publishing, 256 p.

Parfitt, E.A., Wilson, L., and Neal, C.A., 1995, Factors influencing the height of Hawaiian lava fountains; implications for the use of fountain height as an indicator of magma gas content: Bulletin of Volcanology, v. 57, no. 6, p. 440–450, doi:10.1007/BF00300988.

Patrick, M.R., Orr, T.R., Wilson, D., Dow, D., and Freeman, R., 2011a, Cyclic spattering, seismic tremor, and surface fluctuation within a perched lava channel, Kīlauea Volcano: Bulletin of Volcanology, v. 73, no. 6, p. 639–653, doi:10.1007/s00445-010-0431-2.

Patrick, M.R., Wilson, D., Fee, D., Orr, T.R., and Swanson, D.A., 2011b, Shallow degassing events as a trigger for very-long-period seismicity at Kīlauea Volcano, Hawai‘i: Bulletin of Volcanology, v. 73, no. 9, p. 1179–1186, doi:10.1007/s00445-011-0475-y.

Patrick, M., Orr, T.A. Sutton, J., Elias, T., and Swanson, D., 2013, The first five years of Kīlauea’s summit eruption in Halema‘uma‘u Crater, 2008–2013: U.S. Geological Survey Fact Sheet 2013–3116, 4 p., doi:10.3133/fs20133116.

Perret, F.A., 1913a, The lava fountains of Kilauea: American Journal of Science, ser. 4, v. 35, no. 206, art. 14, p. 139–148, doi:10.2475/ajs.s4-35.206.139.

Perret, F.A., 1913b, The circulatory system in the Halemaumau lava lake during the summer of 1911: American Journal of Science, ser. 4, v. 35, no. 208, art. 30, p. 337–349, doi:10.2475/ajs.s4-35.208.337.

Perret, F.A., 1913c, The ascent of lava: American Journal of Science, ser. 4, v. 36, no. 216, art. 53, p. 605–608, doi:10.2475/ajs.s4-36.216.605

Perret, F.A., 1913d, Some Kilauean ejectamenta: American Journal of Science, ser. 4, v. 35, no. 210, art. 52, p. 611–618, doi:10.2475/ajs.s4-35.210.611.

Peterson, D.W., Christiansen, R.L., Duffield, W.A., Holcomb, R.T., and Tilling, R.I., 1976, Recent activity of Kilauea Volcano, Hawaii, *in* Gonzales-Ferran, O., ed., Proceedings of the Symposium on Andean and Antarctic Volcanology Problems, Santiago, Chile, September 9–14, 1974: Napoli, F. Giannini & Figli, International Association of Volcanology and Chemistry of the Earth’s Interior (IAVCEI), special ser., p. 646–656.

Pioli, L., Bonadonna, C., Azzopardi, B.J., Phillips, J.C., and Ripepe, M., 2012, Experimental constraints on the outgassing dynamics of basaltic magmas: Journal of Geophysical Research, v. 117, B03204, 17 p., doi:10.1029/2011JB008392.

Polacci, M., Corsaro, R.A., and Andronico, D., 2006, Coupled textural and compositional characterization of basaltic scoria; insights into the transition from Strombolian to fire fountain activity at Mount Etna, Italy: Geology, v. 34, no. 3, p. 201–204, doi:10.1130/G22318.1.

Poland, M.P., Miklius, A., Orr, T.R., Sutton, A.J., Thornber, C.R., and Wilson, D., 2008, New episodes of volcanism at Kilauea Volcano, Hawaii: Eos (American Geophysical Union Transactions), v. 89, no. 5, p. 37–38, doi:10.1029/2008EO050001.

Poland, M.P., Miklius, A., Sutton, A.J., and Thornber, C.R., 2012, A mantle-driven surge in magma supply to Kīlauea Volcano during 2003–2007: Nature Geoscience, v. 5, no. 4, p. 295–300, doi:10.1038/ngeo1426.

Pollard, D.D., 1973, Derivation and evaluation of a mechanical model for sheet intrusions: Tectonophysics, v. 19, no. 3, p. 233–269, doi:10.1016/0040-1951(73)90021-8.

Pollard, D.D., Segall, P., and Delaney, P.T., 1982, Formation and interpretation of dilatant echelon cracks: Geological Society of America Bulletin, v. 93, no. 12, p. 1291–1303, doi:10.1130/0016-7606(1982)93<1291:FAIODE>2.0.CO;2.

Potuzak, M., Nichols, A.R.L., Dingwell, D.B., and Clague, D.A., 2008, Hyperquenched volcanic glass from Loihi Seamount, Hawaii: Earth and Planetary Science Letters, v. 270, nos. 1–2, p. 54–62, doi:10.1016/j.epsl.2008.03.018.

Powers, H.A., 1948, A chronology of the explosive eruptions of Kilauea: Pacific Science, v. 2, no. 4, p. 278–292. [Also available at http://hdl.handle.net/10125/9067.]

Powers, S., 1916, Explosive ejectamenta of Kilauea: American Journal of Science, ser. 4, v. 41, no. 243, art. 12, p. 227–244, doi:10.2475/ajs.s4-41.243.227.

Proussevitch, A.A., Sahagian, D.L., and Kutolin, V.A., 1993, Stability of foams in silicate melts: Journal of Volcanology and Geothermal Research, v. 59, nos. 1–2, p. 161–178, doi:10.1016/0377-0273(93)90084-5.

Ramani, M.V., Kumar, R., and Gandhi, K.S., 1993, A model for static foam drainage: Chemical Engineering Science, v. 48, no. 3, p. 455–465, doi:10.1016/0009-2509(93)80300-F.

Richter, D.H., and Moore, J.G., 1966, Petrology of the Kilauea Iki lava lake, Hawaii, *in* The 1959–60 eruption of Kilauea volcano, Hawaii: U.S. Geological Survey Professional Paper 537–B, p. B1–B26. [Also available at http://pubs.usgs.gov/pp/0537/report.pdf.]

Richter, D.H., and Murata, K.J., 1966, Petrography of the lavas of the 1959–60 eruption of Kilauea Volcano, Hawaii, *in* The 1959–60 eruption of Kilauea volcano, Hawaii: U.S. Geological Survey Professional Paper 537–D, p. D1–D12. [Also available at http://pubs.usgs.gov/pp/0537/report.pdf.]

Richter, D.H., Eaton, J.P., Murata, J., Ault, W.U., and Krivoy, H.L., 1970, Chronological narrative of the 1959–60 eruption of Kilauea Volcano, Hawaii, *in* The 1959–60 eruption of Kilauea volcano, Hawaii: U.S. Geological Survey Professional Paper 537–E, p. E1–E73. [Also available at http://pubs.usgs.gov/pp/0537e/report.pdf.]

Rubin, A.M., 1993, Tensile fracture of rock at high confining pressure; implications for dike propagation: Journal of Geophysical Research, v. 98, no. B9, p. 15919–15935, doi:10.1029/93JB01391.

Rubin, A.M., and Pollard, D.D., 1987, Origins of blade-like dikes in volcanic rift zones, chap. 53 *of* Decker, R.W., Wright, T.L., and Stauffer, P.H., eds., Volcanism in Hawaii: U.S. Geological Survey Professional Paper 1350, v. 2, p. 1449–1470. [Also available at http://pubs.usgs.gov/pp/1987/1350/.]

Rust, A.C., and Cashman, K.V., 2011, Permeability controls on expansion and size distributions of pyroclasts: Journal of Geophysical Research, v. 116, B11202, 17 p., doi:10.1029/2011JB008494.

Rust, A.C., and Manga, M., 2002, Effects of bubble deformation on the viscosity of dilute suspensions: Journal of Non-Newtonian Fluid Mechanics, v. 104, no. 1, p. 53–63, doi:10.1016/S0377-0257(02)00013-7.

Ryan, M.P., 1988, The mechanics and three-dimensional internal structure of active magmatic systems; Kilauea volcano, Hawaii: Journal of Geophysical Research, v. 93, no. B5, p. 4213–4248, doi:10.1029/JB093iB05p04213.

Sable, J.E., Houghton, B.F., Del Carlo, P., and Coltelli, M., 2006, Changing conditions of magma ascent and fragmentation during the Etna 122 BC basaltic Plinian eruption; evidence from clast microtextures: Journal of Volcanology and Geothermal Research, v. 158, nos. 3–4, p. 333–354, doi:10:1016/j.jvolgeores.2006.07.006.

Sahagian, D.L., 1985, Bubble migration and coalescence during the solidification of basaltic lava flows: Journal of Geology, v. 93, no. 2, p. 205–211, doi:10.1086/628942.

Sahagian, D.L., Anderson, A.T., and Ward, B., 1989, Bubble coalescence in basalt flows; comparison of a numerical model with natural examples: Bulletin of Volcanology, v. 52, no. 1, p. 49–56, doi:10.1007/BF00641386.

Sarda, P., and Graham, D., 1990, Mid-ocean ridge popping rocks; implications for degassing at ridge crests: Earth and Planetary Science Letters, v. 97, nos. 3–4, p. 268–289, doi:10.1016/0012-821X(90)90047-2.

Scriven, L.E., 1959, On the dynamics of phase growth: Chemical Engineering Science, v. 10, nos. 1–2, p. 1–13, doi:10.1016/0009-2509(59)80019-1.

Seyfried, R., and Freundt, A., 2000, Experiments on conduit flow and eruption behavior of basaltic volcanic eruptions: Journal of Geophysical Research, v. 105, no. B10, p. 23727–23740, doi:10.1029/2000JB900096.

Shaw, H.R., 1972, Viscosities of magmatic silicate liquids; an empirical method of prediction: American Journal of Science, v. 272, no. 9, p. 870–893, doi:10.2475/ajs.272.9.870.

Shaw, H.R., Wright, T.L., Peck, D.L., and Okamura, R., 1968, The viscosity of basaltic magma; an analysis of field measurements in Makaopuhi lava lake, Hawaii: American Journal of Science, v. 266, no. 4, p. 225–264, doi:10.2475/ajs.266.4.225.

Shepherd, E.S., 1938, The gases in rocks and some related problems: American Journal of Science, ser. 5, v. 35–A (The Arthur L. Day volume), p. 311–351, accessed May 5, 2013, at http://earth.geology.yale.edu/~ajs/1938-A/311.pdf.

Shimozuru, D., 1978, Dynamics of magma in a volcanic conduit—Special emphasis on viscosity of magma with bubbles: Bulletin Volcanologique, v. 41, no. 4, p. 333–340, doi:10.1007/BF02597368.

Sonin, A.A., Bonfillon, A., and Langevin, D., 1994, Thinning of soap films; the role of surface viscoelasticity: Journal of Colloid and Interface Science, v. 162, no. 2, p. 323–330, doi:10.1016/j.jvolgeores.2007.07.020.

Sparks, R.S.J., 1978, The dynamics of bubble formation and growth in magmas; a review and analysis: Journal of Volcanology and Geothermal Research, v. 3, nos. 1–2, p. 1–37, doi:10.1016/0377-0273(78)90002-1.

Sparks, R.S.J., and Wilson, L., 1976, A model for the formation of ignimbrite by gravitational column collapse: Journal of the Geological Society of London, v. 132, no. 4, p. 441–451, doi:10.1144/gsjgs.132.4.0441.

Sparks, R.S.J., Bursik, M.I., Carey, S.N., Gilbert, J.S., Glaze, L.S., Sigurdsson, H., and Woods, A.W., 1997, Volcanic plumes: Chichester, U.K., John Wiley and Sons, 590 p.

Spera, F.J., 2000, Physical properties of magma, *in* Sigurdsson, H., Houghton, B.F., McNutt, S.R., Rymer, H., and Styx, J., eds., Encyclopedia of volcanoes: San Diego, Calif., Academic Press, p. 171–190.

Stearns, H.T., 1939, Geologic map and guide of the island of Oahu, Hawaii (with a chapter on mineral resources): Hawaii Division of Hydrography Bulletin 2, 75 p., scale 1:62,500.

Stearns, H.T., and Vaksvik, K.N., 1935, Geology and ground-water resources of the island of Oahu, Hawaii: Hawaii Division of Hydrography Bulletin 1, 479 p. [Also available at http://pubs.usgs.gov/misc/stearns/Oahu.pdf.]

Stein, D.J., and Spera, F.J., 1992, Rheology and microstructure of magmatic emulsions; theory and experiments: Journal of Volcanology and Geothermal Research, v. 49, nos. 1–2, p. 157–174, doi:10.1016/0377-0273(92)90011-2.

Stone, J.B., 1926, The products and structure of Kilauea: Honolulu, Bernice P. Bishop Museum Bulletin 33, 59 p.

Stothers, R.B., Wolff, J.A., Self, S., and Rampino, M.R., 1986, Basaltic fissure eruptions, plume heights, and atmospheric aerosols: Geophysical Research Letters, v. 13, no. 8, p. 725–728, doi:10.1029/GL013i008p00725.

Stovall, W.K., Houghton, B.F., Gonnermann, H., Fagents, S.A., and Swanson, D.A., 2011, Eruption dynamics of Hawaiian-style fountains; the case study of episode 1 of the Kīlauea Iki 1959 eruption: Bulletin of Volcanology, v. 73, no. 5, p. 511–529, doi:10.1007/s00445-010-0426-z.

Stovall, W.K., Houghton, B.F., Hammer, J.E., Fagents, S.A., and Swanson, D.A., 2012, Vesiculation of high fountaining Hawaiian eruptions; episodes 15 and 16 of 1959 Kīlauea Iki: Bulletin of Volcanology, v. 74, no. 2, p. 441–455, doi:10.1007/s00445-011-0531-7.

Suckale, J., Hagar, B.H., Elkins-Tanton, L.T., and Nave, J.-C., 2010, It takes three to tango; 2. Bubble dynamics in basaltic volcanoes and ramifications for modeling normal Strombolian activity: Journal of Geophysical Research, v. 115, B07410, 17 p., doi:10.1029/2009JB006917.

Sutton, A.J., and Elias, T., 2014, One hundred volatile years of volcanic gas studies at HVO, chap. 7 *of* Poland, M.P., Takahashi, T.J., and Landowski, C.M., eds., Characteristics of Hawaiian volcanoes: U.S. Geological Survey Professional Paper 1801 (this volume).

Sutton, A.J., Elias, T., and Kauahikaua, J.P., 2003, Lava-effusion rates for the Pu‘u ‘Ō‘ō-Kūpaianaha eruption derived from SO_2 emissions and very low frequency (VLF) measurements, *in* Heliker, C.C., Swanson, D.A., and Takahashi, T.J., eds., The Pu‘u ‘Ō‘ō-Kūpaianaha eruption of Kīlauea Volcano, Hawai‘i; the first 20 years: U.S. Geological Survey Professional Paper 1676, p. 137–148. [Also available at http://pubs.usgs.gov/pp/pp1676.]

Swanson, D.A., and Christiansen, R.L., 1973, Tragic base surge in 1790 at Kilauea Volcano: Geology, v. 1, no. 2, p. 83–86, doi:10.1130/0091 7613(1973)1<83:TBSIAK>2.0.CO;2.

Swanson, D.A., Duffield, W.A., Jackson, D.B., and Peterson, D.W., 1979, Chronological narrative of the 1969–71 Mauna Ulu eruption of Kilauea Volcano, Hawaii: U.S. Geological Survey Professional Paper 1056, 55 p., 4 pls. [Also available at http://pubs.usgs.gov/pp/1056/report.pdf.]

Swanson, D.A., Fiske, D., Rose, T.R., Houghton, B., and Mastin, L., 2011, Kīlauea—an explosive volcano in Hawai‘i: U.S. Geological Survey Fact Sheet 2011–3064, 4 p. [Also available at http://pubs.usgs.gov/fs/2011/3064/fs2011-3064.pdf.]

Swanson, D.A., Rose, T.R., Fiske, R.S., and McGeehin, J.P., 2012a, Keanakāko‘i Tephra produced by 300 years of explosive eruptions following collapse of Kīlauea's caldera in about 1500 CE: Journal of Volcanology and Geothermal Research, v. 215–216, February 15, p. 8–25, doi:10.1016/j.jvolgeores.2011.11.009.

Swanson, D.A., Rose, T.R, Mucek, A.G., Garcia, M.O., Fiske, R.S., and Mastin, L.G., 2014, Cycles of explosive and effusive eruptions at Kīlauea Volcano, Hawai‘i; Geology, v. 42, no. 7, p. 631–634, doi:10.1130/G35701.1.

Tilling, R.I., Christiansen, R.L., Duffield, W.A., Endo, E.T., Holcomb, R.T., Koyanagi, R.Y., Peterson, D.W., and Unger, J.D., 1987, The 1972–1974 Mauna Ulu eruption, Kilauea Volcano; an example of quasi-steady-state magma transfer, chap. 16 *of* Decker, R.W., Wright, T.L., and Stauffer, P.H., eds., Volcanism in Hawaii: U.S. Geological Survey Professional Paper 1350, v. 1, p. 405–469. [Also available at http://pubs.usgs.gov/pp/1987/1350/.]

Toramaru, A., 1989, Vesiculation process and bubble size distributions in ascending magmas with constant velocities: Journal of Geophysical Research, v. 94, no. B12, p. 17523–17542, doi:10.1029/JB094iB12p17523.

Toramaru, A., 1990, Measurement of bubble size distributions in vesiculated rocks with implications for quantitative estimation of eruption processes: Journal of Volcanology and Geothermal Research, v. 43, nos. 1–4, p. 71–90, doi:10.1016/0377-0273(90)90045-H.

Underwood, E.E., 1970, Quantitative stereology: Reading, Mass., Addison-Wesley, 274 p.

Vergniolle, S., 1996, Bubble size distribution in magma chambers and dynamics of basaltic eruptions: Earth and Planetary Science Letters, v. 140, nos. 1–4, p. 269–279, doi:10.1016/0012-821X(96)00042-8.

Vergniolle, S., 2008, From sound waves to bubbling within a magma reservoir; comparison between eruptions at Etna (2001, Italy) and Kilauea (Hawaii), *in* Lane, S.J., and Gilbert, J.S., eds., Fluid motions in volcanic conduits; a source of seismic and acoustic signals: Geological Society of London Special Publication 307, p. 125–146, doi:10.1144/SP307.8.

Vergniolle, S., and Jaupart, C., 1986, Separated two-phase flow and basaltic eruptions: Journal of Geophysical Research, v. 91, no. B12, p. 12842–12860, doi:10.1029/JB091iB12p12842.

Vergniolle, S., and Jaupart, C., 1990, Dynamics of degassing at Kilauea Volcano, Hawaii: Journal of Geophysical Research, v. 95, no. B3, p. 2793–2809, doi:10.1029/JB095iB03p02793.

Verhoogen, J., 1951, Mechanics of ash formation: American Journal of Science, v. 249, no. 10, p. 729–739, doi:10.2475/ajs.249.10.729.

Volkov, V.P., and Ruzaykin, G.I., 1975, Equilibrium calculations in volcanic gaseous systems: Bulletin Volcanologique, v. 39, no. 1, p. 47–63, doi:10.1007/BF02596945.

Walker, G.P.L., 1987, The dike complex of Koolau Volcano, Oahu; internal structure of a Hawaiian rift zone, chap. 41 *of* Decker, R.W., Wright, T.L., and Stauffer, P.H., eds., Volcanism in Hawaii: U.S. Geological Survey Professional Paper 1350, v. 2, p. 961–993. [Also available at http://pubs.usgs.gov/pp/1987/1350/.]

Walker, G.P.L., Wilson, L., and Bowell, E.L.G., 1971, Explosive volcanic eruptions— I. The rate of fall of pyroclasts: Geophysical Journal of the Royal Astronomical Society, v. 22, no. 4, p. 377–383, doi:10.1111/j.1365-246X.1971.tb03607.

Watson, E.B., Sneeringer, M.A., and Ross, A., 1982, Diffusion of dissolved carbonate in magmas; experimental results and applications: Earth and Planetary Sciences Letters, v. 61, no. 2, p. 346–358, doi:10.1016/0012-821X(82)90065-6.

Weaire, D., and Phelan, R., 1994, A counter example to Kelvin's conjecture on minimal surfaces: Philosophical Magazine Letters, v. 69, no. 2, p. 107–110, doi:10.1080/09500839408241577.

Wentworth, C.K., 1938, Ash formations of the island Hawaii; third special report of the Hawaiian Volcano Observatory of Hawaii National Park and the Hawaiian Volcano Research Association: Honolulu, Hawaiian Volcano Research Association, 183 p. (Reprinted in Bevens, D., Takahashi, T.J., and Wright, T.L., eds., 1988, The early serial publications of the Hawaiian Volcano Observatory: Hawaii National Park, Hawaii, Hawai‘i Natural History Association, v. 1, p. 144–334.)

Wentworth, C.K., and Jones, A.E., 1940, Intrusive rocks of the leeward slope of the Koolau Range, Oahu: Journal of Geology, v. 48, no. 8, pt. 2, p. 975–1006, doi:10.1086/624933.

Wentworth, C.K., and Macdonald, G.A., 1953, Structures and forms of basaltic rocks in Hawaii: U.S. Geological Survey Bulletin 994, 98 p. [Also available at http://pubs.usgs.gov/bul/0994/report.pdf.]

Wilson, L., 1999, Explosive volcanic eruptions—X. The influence of pyroclast size distributions and released magma gas contents on the eruption velocities of pyroclasts and gas in Hawaiian and Plinian eruptions: Geophysical Journal International, v. 136, no. 3, p. 609–619, doi:10.1046/j.1365-246x.1999.00750.x.

Wilson, L,, and Head, J.W., III, 1981, Ascent and eruption of basaltic magma on the Earth and Moon: Journal of Geophysical Research, v. 86, no. B4, p. 2971–30001, doi:10.1029/JB086iB04p02971.

Wilson, L., and Head, J.W., III, 1988, Nature of local magma storage zones and geometry of conduit systems below basaltic eruptions sites; Pu'u 'O'o, Kilauea east rift, Hawaii, example: Journal of Geophysical Research, v. 93, no. B12, p. 14785–14792, doi:10.1029/JB093iB12p14785.

Wilson, L., Sparks, R.S.J., Huang, T.C., and Watkins, N.D., 1978, The control of volcanic column heights by eruption energetics and dynamics: Journal of Geophysical Research, v. 83, no. B4, p. 1829–1836, doi:10.1029/JB083iB04p01829.

Wilson, L., Parfitt, E.A., and Head, J.W., III, 1995, Explosive volcanic eruptions—VIII. The role of magma recycling in controlling the behavior of Hawaiian-style lava fountains: Geophysical Journal International, v. 121, no. 1, p. 215–225, doi:10.1111/j.1365-246X.1995.tb03522.x.

Wolfe, E.W., Garcia, M.O., Jackson, D.B., Koyanagi, R.Y., Neal, C.A., and Okamura, A.T., 1987, The Puu Oo eruption of Kilauea Volcano, episodes 1–20, January 3, 1983, to June 8, 1984, chap. 17 *of* Decker, R.W., Wright, T.L., and Stauffer, P.H., eds., Volcanism in Hawaii: U.S. Geological Survey Professional Paper 1350, v. 1, p. 471–508. [Also available at http://pubs.usgs.gov/pp/1987/1350/.]

Wolfe, E.W., Neal, C.R., Banks, N.G., and Duggan, T.J., 1988, Geologic observations and chronology of eruptive events, chap. 1 *of* Wolfe, E.W., ed., The Puu Oo eruption of Kilauea Volcano, Hawaii; episodes 1 through 20, January 3, 1983, through June 8, 1984: U.S. Geological Survey Professional Paper 1463, p. 1–98. [Also available at http://pubs.usgs.gov/pp/1463/report.pdf.]

Woods, A.W., 1993, A model of the plumes above basaltic fissure eruptions: Geophysical Research Letters, v. 20, no. 12, p. 1115–1118, doi:10.1029/93GL01215.

Woods, A.W., and Bursik, M.I., 1991, Particle fallout, thermal disequilibrium and volcanic plumes: Bulletin of Volcanology, v. 53, no. 7, p. 559–570, doi:10.1007/BF00298156.

Woods, A.W., and Cardoso, S.S.S., 1997, Triggering basaltic volcanic eruptions by bubble-melt separation: Nature, v. 385, no. 66, p. 518–520, doi:10.1038/385518a0.

Wright, T.L., and Fiske, R.S., 1971, Origin of the differentiated and hybrid lavas of Kilauea Volcano, Hawaii: Journal of Petrology, v. 12, no. 1, p. 1–65, doi:10.1093/petrology/12.1.1.

Wright, T.L., and Okamura, R.T., 1977, Cooling and crystallization of tholeiitic basalt, 1965 Makaopuhi lava lake, Hawaii: U.S. Geological Survey Professional Paper 1004, 78 p. [Also available at http://pubs.usgs.gov/pp/1004/report.pdf.]

Wylie, J.J., Helfrich, K.R., Dade, B., Lister, J.R., and Salzig, J.F., 1999, Flow localization in fissure eruptions: Bulletin of Volcanology, v. 60, no. 6, p. 432–440, doi:10.1007/s004450050243.

Zhang, Y., and Stolper, E.M., 1991, Water diffusion in a basaltic melt: Nature, v. 351, no. 6324, p. 306–309, doi:10.1038/351306a0.